THE EFFECT OF TEMPERATURE ON

UNBONDED FIBER-REINFORCED ELASTOMERIC ISOLATORS

THE EFFECT OF TEMPERATURE ON UNBONDED FIBER-REINFORCED ELASTOMERIC ISOLATORS

By

ALEXANDER SCIASCETTI, B.Eng.Mgmt.

A Thesis Submitted to the School of Graduate Studies in Partial Fulfilment of the Requirements for the Degree Master of Applied Science

McMaster University

© Copyright Alexander Sciascetti, 2017

Master of Applied Science (2017)
(Civil Engineering)

McMaster University
Hamilton, Ontario

Title: The Effect of Temperature on
Unbonded Fiber-Reinforced Elastomeric Isolators

Author: Alexander Sciascetti

Supervisor: Dr. Michael J. Tait

Number of Pages: x, 111

ABSTRACT

During strong ground motions, structures equipped with base isolation systems have been shown to have their seismic demand significantly reduced, mitigating adverse effects such as damage and loss of life. More recently, the fiber-reinforced elastomeric isolator (FREI) has been investigated as a relatively new type of isolator for the base isolation of structures. Constructed from alternating layers of elastomer and carbon-fiber cloth, FREI can be produced in large pads that can be cut to any desired size and shape when required.

In bridges, FREI can to be used in an unbonded application (U-FREI) by placing them between the bridge deck and the piers. Experimental and numerical investigations have shown U-FREI as a viable option for the isolation of bridges. However, experimental studies have been limited to room temperature testing. In North America, climates vary drastically across the continent. Northern climates, such as those existent in Canada, are capable of reaching extremely low temperatures. Thus, base isolated bridges in these regions require isolation systems that perform adequately at cold temperatures.

The studies presented in this dissertation have been completed in order to investigate the effects that low temperatures have on U-FREI used in bridge structures. An experimental program was conducted that evaluated the behaviour of U-FREI. It was found that U-FREI performed adequately under lateral displacements expected during a seismic event, and provided acceptable response under vertical and rotational testing that is typical of normal bridge operation. Using these results, a numerical model for U-FREI was then updated to account for the effects of low temperature. The model was combined with a bridge model to evaluate the seismic response of a bridge structure isolated with U-FREI subjected to low temperatures. A substantial reduction in seismic demand was achieved, even under the most severe conditions tested.

ACKNOWLEDGEMENTS

First, I would like to thank my supervisor, Dr. Tait, for his advice and guidance, and his genuine interest in my personal success throughout my degree. Thank you as well to Yasser Al-Anany for his advice and for teaching me how to construct my specimens, run the test setup, and aiding me in my low temperature tests.

In the lab, Paul Heerema and Kent Wheeler provided me with all the help and guidance I could ask for. Even when things weren't going as I had planned, they made me enjoy my time in the lab and I'm very appreciative of that.

My degree would not have been as enjoyable without my friends and colleagues, Kevin McNamara, Bryanna Noade, Paul Steneker, and Matt Ficara. Thank you for your help during testing, letting me bounce ideas off of you and listening to me complain. Mostly, thank you for making me remember that it's okay (and beneficial) to take time away from my research and writing for a night out with friends every once in a while.

Finally, I want to give a big thank you to my family for their love, unwavering support and encouragement in pursuing my dreams. A most special thank you to Diana Gresku, who always believed in me and was there for me anytime I needed.

TABLE OF CONTENTS

LIST OF TABLES

LIST OF FIGURES

DECLARATION OF ACADEMIC ACHIEVEMENT

The research and analysis presented herein was completed solely by Alexander Sciascetti under the guidance and supervision of Dr. Michael Tait. All external sources of information have been cited where applicable. This dissertation, for submission in partial fulfilment of the requirements for the degree of Master of Applied Science, has been prepared as a compilation of two scholarly works. As a result, there may be some overlap of the information presented in the introductory sections of this dissertation and the scholarly works.

Chapter 2 The Effect of Temperature on the Lateral, Vertical and Rotational Response of Unbonded Fiber-Reinforced Elastomeric Isolators

Sciascetti, A. and Tait, M.J.

The preparation of the setup and specimens, the experimental tests and the analysis of data were completed by Alexander Sciascetti under the supervision of Dr. Michael Tait. The resulting scholarly article was written by Alexander Sciascetti with modifications made under the direction of Dr. Michael Tait.

Chapter 3 The Effect of Temperature on the Seismic Performance of a Structure Isolated with Unbonded Fiber-Reinforced Elastomeric Isolators

Sciascetti, A. and Tait, M.J.

The updated FREI numerical model, the bridge model and all simulations, and the data analysis were completed by Alexander Sciascetti under the supervision of Dr. Michael Tait. The resulting scholarly article was written by Alexander Sciascetti with modifications made under the direction of Dr. Michael Tait.

CHAPTER 1

INTRODUCTION

During seismic events, base isolation systems are used to uncouple structures from the motion of the ground, which allows the adverse effects of earthquakes to be mitigated. Isolation systems introduce a layer that is flexible in the horizontal direction, but stiff vertically in order to support the weight of the structure above. The low lateral stiffness of the isolation system results in a low natural frequency of the structure that is often shifted away from the prevalent frequencies of seismically induced ground motions (Yang et al. 2003). This results in a reduction of the seismic demand on the structure, but an increase in displacement. Isolators can have some energy dissipation in order to aid in limiting the systems displacement response at resonance.

1.1 ISOLATION SYSTEMS

Early examples of base isolation systems include the idea to use layers of talc or cast-iron balls placed between the structure and foundation (Kelly and Naeim 1999). These methods make use of static and kinetic friction properties. During an earthquake, static friction is overcome and the layers of talc are able to slide past one another, preventing the structure from experiencing large accelerations at the expense of large displacements.

1.1.1 Friction Pendulum System

More recently, friction pendulum isolation systems (FPS) have been developed. These systems are comprised of multiple isolators that, in the most basic system,

contain two main pieces: a concave steel surface and an articulated slider (Zayas et al. 1990). The slider moves along the concave surface in order to accommodate displacements. The coefficient of friction of the surface can be changed in order to provide different levels of energy dissipation and to define the force required to initiate sliding, while the radius of the concave surface dictates the natural period of the system (Zayas et al. 1990). The restoring force for each isolator is provided by the mass of the structure above as the slider moves to an elevated positon along the concave surface (Kelly and Naeim 1999).

1.1.2 Elastomeric Isolation Systems

The development of multilayer elastomeric isolation systems has allowed base isolation to become more widespread over the last thirty years (Kelly and Konstantinidis 2011). These isolators have alternating layers of elastomer, which control the isolators' lateral response, and rigid steel plates, which increase the vertical stiffness of the bearing. The inclusion of steel shims allows the bulging of the elastomer layers to be controlled and enables a larger shape factor to be achieved. Often denoted as *S*, the shape factor is the ratio of the loaded area of a single elastomer layer in the bearing to the unloaded area, or the area of the elastomer layer that is able to bulge outwards during loading (Kelly and Konstantinidis 2011). The shape factor controls the compression modulus, which in turn is used to calculate vertical stiffness. Having a large vertical stiffness is important as it allows gravity loads to be transferred from the structure to its foundation without significant vertical displacements. In the case of a bridge that experiences varying loads, a high vertical stiffness will prevent the bridge

from excessive vertical motion as vehicles of different sizes traverse it. With regards to the lateral response of these elastomeric isolators, the rubber layers allow for the isolator to accommodate lateral displacements between the bridge and substructure (Yang et al. 2003). These displacements can be in response to temperature induced contraction and expansion, or from ground motion.

Elastomeric isolators are typically separated into three categories comprised of low-damping rubber (LDR), lead-plug rubber (LPR), and high-damping rubber (HDR) isolators (Kelly and Naeim 1999). LDR isolators typically have low damping and as a result, can behave nearly linearly in shear (Kelly and Naeim 1999). These isolators can be combined with systems of supplementary devices that add damping, such as viscous dampers. LPR isolators are similar to LDR isolators, but have increased damping properties due to the addition of one or more lead-plugs that are inserted snuggly into holes in the isolator. Each lead-plug is forced to deform in shear as the isolator deforms and provides the isolator with additional energy dissipation, as well as a bilinear response (Kelly and Naeim 1999). The damping that is provided by HDR isolators is inherent to the rubber compound used in the isolator. The elastomer is produced with the addition of carbon black and other proprietary additives that increase damping, while increasing other properties such as tear resistance (Goodyear Tire & Rubber Company 2004). However, the mechanical properties of HDR isolators are typically highly nonlinear (Burtscher and Dorfmann 2004).

1.2 FIBER-REINFORCED ELASTOMERIC ISOLATOR

A more recent development in base isolation research introduces an elastomeric isolator similar to that of a LDR isolator, but with one main difference; the rigid steel shims that are used to provide vertical stiffness are replaced with much more flexible layers of carbon fiber cloth. Fiber-reinforced elastomeric isolators (FREI) have been investigated due to their potential to be a lighter and cost-effective alternative to typical steel-reinforced elastomeric isolators (SREI). By replacing the steel shim layers with carbon fiber of similar elastic modulus, it has been found that the required vertical stiffness of the isolator can still be achieved (Moon et al. 2002; Al-Anany et al. 2016). The reduction in flexural rigidity has also been shown to be negligible in affecting the horizontal stiffness of bonded FREI. Bonded refers to the attachment of the isolator to the foundation below and the structure above. In comparison, FREI only exhibit a reduction on the order of 10% when compared to SREI (Kelly 1999).

1.2.1 Energy Dissipation

The flexibility of the carbon fiber layers enables FREI to be used in an unbonded application (U-FREI). This means that U-FREI can be placed between the foundation and structure, without the need to be fastened in place. They are able to exhibit desirable properties as a result. One such characteristic is that U-FREI have a greater damping ratio than that of the elastomer itself (Toopchi-Nezhad et al. 2008a). It has been hypothesized that as the isolator is displaced laterally, the flexible fiber-reinforcement bends and the individual fibers in the reinforcement slip past each other in order to allow the movement (Kelly and Naeim 1999; Toopchi-Nezhad et al. 2008a).

Frictional forces that develop during vertical loading as tension is increased in the fibers resist this movement. Slip occurs as the frictional forces between the fibers are overcome and as a result, energy is dissipated in excess of the amount dissipated by the elastomer compound.

1.2.2 Rollover

Another property of U-FREI can be seen at larger shear strains when an appropriate aspect ratio is used (Toopchi-Nezhad et al. 2008b). The aspect ratio is the ratio of the width to the total height of the bearing. The desired ratio can be easily achieved due to the ease of which FREI can be cut to size from a larger pad (Toopchi-Nezhad et al. 2008a; Sciascetti et al. 2016). As the U-FREI is subjected to increasing lateral displacement, the faces in contact with the horizontal loading supports begin to lift off and a rollover mechanism begins to develop (Toopchi-Nezhad et al. 2008b). The mechanism is depicted in Figure 1.1. This initial change in boundary conditions results in a reduction in effective lateral stiffness that continues to decrease as displacements are increased. At very large lateral displacements an increase in lateral stiffness is observed. It is attributed to the FREI exhibiting full rollover. The originally vertical faces of the bearing become horizontal and in full contact with the upper and lower loading plates.

1.2.3 Full Rollover

A mathematical model developed by Kelly and Konstantinidis (2007) predicts the onset of full rollover for isolators constructed with thin steel reinforcing shims, which are assumed to be fully flexible in flexure. Two other main assumptions were

detailed. The model assumes that the elastomer is incompressible and that once rollover occurs, the isolator surfaces that roll off of the supports are stress free. Extending the first assumption to the use of fiber reinforcement allows the use of the model to estimate full rollover for U-FREI. This occurrence is at a lateral displacement equal to approximately 5/3 the height of the isolator. This approximation is affected by the elastic modulus of the reinforcement material in bending. As the modulus is increased, compared to that of the elastic modulus of the elastomer in bending, the onset of full rollover is delayed and occurs at larger lateral displacements (Van Engelen et al. 2014a). Full rollover is significant as it acts to limit the maximum lateral displacement of the U-FREI and prevents a negative lateral tangential stiffness from occurring (de Raaf et al. 2011). When the lateral tangential stiffness remains positive throughout the entire hysteresis loop, the rollover mechanism is deemed stable and the isolators are referred to as Stable Unbonded Fiber-Reinforced Elastomeric Isolators (SU-FREI) (Toopchi-Nezhad et al. 2008a). In a study completed by Van Engelen et al. (2014), stability was found to be directly related to the aspect ratio of the bearing. It was determined that aspect ratios greater than 2.5 results in U-FREI stability being maintained. This was also confirmed analytically by Toopchi-Nezhad (2014). When the aspect ratio is greater than 10, it was found that U-FREI can be instead modeled with a constant effective stiffness, ignoring the rollover mechanism (Van Engelen et al. 2014a).

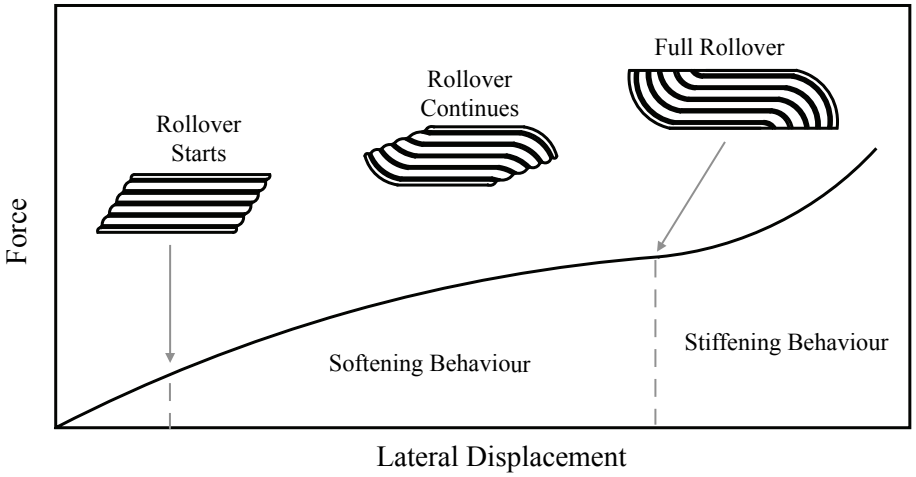

Figure 1.1: Phases of U-FREI load-displacement curve depicting rollover.

1.2.4 Vertical and Rotational Response

There has also been research completed on the vertical and rotational responses of U-FREI. Toopchi-Nezhad et al. (2008b) found that U-FREI provided an adequately high vertical stiffness. This was later confirmed with a parametric study on ¼ scale U-FREI, where the vertical stiffness was at least 20 times greater than required when compared to the maximum expected frequency of the base isolated building (Toopchi-Nezhad et al. 2009). In addition, the vertical stiffness did not degrade significantly after lateral cyclic loading. Van Engelen et al. (2014b) modified bearings by placing holes in the loading surface. It was found that even with holes of small diameter, the vertical stiffness was reduced. This was due to the effect that the removal of a small amount of area can have on the shape factor of the FREI and is consistent with that of SREI.

The rotational behaviour of U-FREI compared to bonded FREI has been investigated both numerically and experimentally (Al-Anany and Tait 2015, 2016). In both of these studies, the unbonded FREI outperformed the bonded variant by reducing

the stress demand on the elastomer and accommodating large angles of rotation. These studies were followed by further research assessing the viability of FREI as bearings for bridge applications (Al-Anany and Tait 2017a, 2017b). The U-FREI remained stable during cyclic rotational testing, as would be induced by a bridge deck or girder. Lateral offsets, on magnitude with expectations for a bridge bearing, did not significantly affect the vertical response.

1.3 U-FREI MODELING

As a result of the rollover mechanism that U-FREI exhibit, numerically modelling the lateral behaviour of the isolators was initially challenging. Early models proposed by Toopchi-Nezhad et al. (2009) required iterative procedures for implementation. Sets of parameters were obtained by fitting the model to experimental hysteresis loops at different displacement amplitudes. Time history analysis was then conducted with the parameters corresponding with an estimated maximum displacement. When the maximum displacement differed from the estimate, interpolation was used to determine the parameters at that displacement amplitude. The analysis would be run again, until the maximum displacement converged. The effectiveness of this approach was found to be dependent on the input ground motion (Toopchi-Nezhad et al. 2009).

Osgooei et al. (2017) proposed a Pivot-Elastic model that eliminated the need for iteration during analysis. This model combines two existing models in parallel to provide the lateral hysteretic behaviour of U-FREI. The first is a bilinear pivot hysteretic model developed by Dowell et al. (1998) and the second is a non-linear

elastic spring defined by a fifth-order polynomial. In total, only six parameters were required for a single U-FREI. The parameters were determined by minimizing the error between the experimental and model values for effective stiffness and effective damping ratio. The effective stiffness and damping values were off by a maximum error of five percent. This method of fitting is simpler than that used for previous proposed models that are fit to the full hysteresis loops obtained from experimental tests. Compared to data obtained through the use of a shake table, results from the Pivot-Elastic model have been found to be in better agreement than results from models proposed by Toopchi-Nezhad et al. (2009).

1.4 IMPACT OF LOW TEMPERATURE

The previous results were gathered at room temperature, but in Canada, bridges experience a wide range of temperatures, especially in cold northern climates. As such, the bearings used in these bridges must be able to withstand the same low temperatures that bridges experience, while still being able to perform adequately. There have been several papers published on how rubber used in bearings performs at low temperatures. The recurring theme is that a stiffening of the rubber is observed (Murrey et al. 1961, Stevenson et al. 1986, Roeder et al. 1990, Yakut and Yura 2002, Sciascetti et al. 2016).

1.4.1 Instantaneous Thermal Stiffening

Roeder et al. (1989) developed a report for the National Cooperative Highway Research Program detailing this low temperature behaviour with respect to elastomeric bridge bearings. It was confirmed that there are two mechanisms that can cause an increase in stiffness due to temperature in elastomers. The first is instantaneous thermal

stiffening, which refers to the rapid change in stiffness of the elastomer when subjected to a change in temperature. This stiffness change is dependent only upon the temperature of the elastomer and occurs almost immediately. As the temperature is decreased and the glass transition temperature of a compound is approached, instantaneous thermal stiffening is amplified greatly. The elastomer transitions into a hard, brittle, glassy state that produces an increase in stiffness that is more that 50 times the room temperature value (Roeder et al. 1989). For natural rubber compounds the transition temperature is at approximately -65°C, while polychloroprene compounds (Neoprene) transition sooner at approximately -55°C.

1.4.2 Low Temperature Crystallization

Low temperature crystallization is the second stiffening mechanism and refers to the change in stiffness associated with the phase transition from an amorphous state to a crystalline state (Bukhina and Kurlyand 2007). When an elastomer is conditioned at a low temperature, nucleation and crystal-growth processes cause the elastomer's structure to become more crystalline. The magnitude of change in stiffness is dependent on the degree of crystallization of the elastomer (Fuller et al. 2004). Once the degree of crystallinity reaches an equilibrium (approximately 30% for natural rubber), the bearing will no longer see an increase in stiffness and the stiffness-time curve will plateau (Stevenson and Maxwell 1986). In their bearing tests, Roeder et al. (1989) also found that the stiffness of the bearings would plateau after long periods of time. As a result of their tests, they recommended 28 days as the longest conditioning period that

an elastomer would need to be subjected to prior to being tested for stiffness increases due to low temperature.

1.4.3 Low Temperature Criteria in Standards

The previously mentioned recommendation from Roeder et al. (1989) and many others are reflected in the AASHTO LRFD Bridge Design Specifications (AASHTO 2012). Roeder et al. (1989) proposed a low temperature map that separated the United States in zones where specific low temperature tests would be required to be completed on bridge bearings. This map was adopted and each zone was paired with a bearing grade that is required for that region. In order to pass the criterion for a given grade, bearings must be less than four times as stiff as their room temperature value after being conditioned at a specified temperature for a specified duration. The bearing grades are given in the AASHTO Standard Specification for Plain and Laminated Elastomeric Bridge Bearings (AASHTO 2016). The criterion for grades 2 through 5 are: -18°C for 7 days, -26°C for 14 days, -37°C for 21 days and -37°C for 28 days. The grade 5 bearing is only required for Alaska.

The low temperature testing criteria has been considered by Yakut and Yura (2002) to be too severe. Through a large experimental program, they found that most of the bearings that failed the testing requirements, could still perform satisfactorily. It was recommended that the zone map be removed and a procedure that accounts for historic temperature records in the service location be used to determine adequate performance instead. This is similar to what is currently in place for cold weather requirements from the Canadian Highway Bridge Design Code (CHBDC). The

CHBDC requires the minimum mean daily temperature for the service location of the bearing to be identified. The bearing would then be subjected to that temperature for a minimum of 14 days (CHBDC 2014).

Guay and Bouaanani (2016) analyzed a large set of historical temperature data taken from Environment Canada. For example, information for a location such as Montreal, Quebec was provided. According to the AASHTO temperature zone map, Montreal would fall within the zone corresponding to a grade 4 bearing (-37°C for 21 days) and the CHBDC would require temperature conditioning for 14 days at a temperature of -31.4°C. Historical data, however, shows that the number of times per year that Montreal is below -25°C for more than 2 days at a time is only once (Guay and Bouaanani 2016). Clearly, the requirements from both codes are not representative of actual conditions in Montreal. Guay and Bouaanani (2016) provided data detailing this occurrence for many cities across Canada and confirmed that the testing criteria for crystallization is too conservative. They provide many city specific curves and generalized contour maps as tools to be used by engineers in order to determine more accurate temperature conditioning requirements.

1.5 OBJECTIVE AND STRUCTURE

In review of the information presented, it can be determined that the low temperature performance of bearings is a subject of great interest. The increase in stiffness of bearings due to instantaneous thermal stiffening and crystallization is a cause of concern for engineers designing bridges and bearings for cold climates. In

Canada, bridge bearings must provide adequate performance at a large range of low temperatures in order limit the shear forces that can be transferred to the supported bridge during a seismic event.

The focus of this research was to investigate the effects of low temperature on unbonded fiber-reinforced elastomeric isolators (U-FREI). After previous research showed the viability of U-FREI as bridge bearings at room temperature, the natural next step was to ensure the ability for these isolators to provide acceptable performance at low temperatures. In order to determine this, the study was split into two sections, experimental and numerical as given below.

Chapter 2 The Effect of Temperature on the Lateral, Vertical and Rotational Response of Unbonded Fiber-Reinforced Elastomeric Isolators
Sciascetti, A and Tait, M.

An experimental investigation was carried out to determine the lateral, vertical and rotational response of U-FREI when subjected to a range of low temperatures and durations. The temperatures and durations that were chosen allowed investigation into the effect of both instantaneous thermal stiffening and crystallization on the isolators. Evaluation of the specimens was completed using the obtained hysteresis loops, as well as the calculated effective stiffness and energy dissipation of each isolator.

Chapter 3 The Effect of Temperature on the Seismic Performance of a Structure Isolated with Unbonded Fiber-Reinforced Elastomeric Isolators
Sciascetti, A and Tait, M.

The acquired data and trends from Chapter 2 were used to update an existing numerical model for U-FREI in order to account for the effect of low temperature. Computer simulations were then completed at various temperatures and durations on a bridge that was isolated using the updated U-FREI model. The bridge was subjected to a suite of ground motions and the response parameters of peak deck displacement, peak deck acceleration and peak pier base shear were used to evaluate performance under different conditions, as well as compared to a non-isolated bridge. This allowed the performance that was determined experimentally for U-FREI at low temperatures to be translated into practicality.

1.6 REFERENCES

AASHTO. 2012. "LRFD Bridge Design Specifications." Washington, D.C.: American Association of State Highway and Transportation Officials.

AASHTO. 2016. "M 251-06 Standard Specification for Plain and Laminated Elastomeric Bridge Bearings." Washington, D.C.: American Association of State Highway and Transportation Officials.

Al-Anany, Y.M., Van Engelen, N.C., and Tait, M.J. 2016. "An Experimental Investigation on the Vertical and Lateral Behaviour of Unbonded Fiber-Reinforced Elastomeric Isolators." *Composites for Construction, under Review*.

Al-Anany, Y.M., and Tait, M.J. 2015. "A Numerical Study on the Compressive and Rotational Behaviour of Fiber Reinforced Elastomeric Isolators (FREI)." *Composite Structures* 133. Elsevier Ltd: 1249–66.

Al-Anany, Y.M., and Tait, M.J. 2016. "An Experimental Study of the Vertical and Rotational Behaviour of Unbonded Fiber- Reinforced Elastomeric Isolators (U-FREI) for Bridge Applications,." *Composites Part B: Engineering*.

Al-Anany, Y.M., and Tait, M.J. 2017a. "Experimental Assessment of Utilizing Fiber Reinforced Elastomeric Isolators as Bearings for Bridge Applications." *Composites Part B: Engineering* 114 (1): 373–85.

Al-Anany, Y.M., and Tait, M.J. 2017b. "Fiber Reinforced Elastomeric Isolators for the Seismic Isolation of Bridges." *Composite Structures* 160. Elsevier Ltd: 300–311.

Bukhina, M.F., and Kurlyand, S.K. 2007. *New Concepts in Polymer Science: Low-Temperature Behaviour of Elastomers*. Boca Raton: CRC Press.

Burtscher, S.L., and Dorfmann, A. 2004. "Compression and Shear Tests of Anisotropic High Damping Rubber Bearings." Engineering Structures 26 (13): 1979–91.

CAN/CSA-S6. 2014. "Canadian Highway Bridge Design Code (CHBDC)." Ontario: Canadian Standard Association.

Dowell, R., Seible, F., and Wilson, E. 1998. "Pivot Hysteresis Model." *ACI Structural Journal* 95 (5).

Fuller, K.N.G., Gough, J., and Thomas, A.G. 2004. "The Effect of Low-Temperature Crystallization on the Mechanical Behavior of Rubber." *Journal of Polymer Science, Part B: Polymer Physics* 42 (11 SPEC. ISS.): 2181–90.

Goodyear Tire & Rubber Company. 2004. *Rubber Compounding*. Edited by Rodgers, B. New York: Marcel Dekker Inc.

Guay, L., and Bouaanani, N. 2016. "Assessment of Low Temperature Exposure for Design and Evaluation of Elastomeric Bridge Bearings and Seismic Isolators in Canada." *Canadian Joural of Civil Engineering* 43: 851–63.

Kelly, J.M., and Naeim, F. 1999. *Design of Seismic Isolated Structures*. New York: John Wiley & Sons, Inc. doi:10.1193/1.1586135.

Kelly, J.M. 1999. "Analysis of Fiber-Reinforced Elastomeric Isolators." *Journal of Seismology and Earthquake Engineering* 2 (1): 19–34.

Kelly, J.M., and Konstantinidis, D. 2007. "Low-Cost Seismic Isolators for Housing in Highly-Seismic Developing Countries." In *10th World Conference on Seismic Isolation, Energy Dissipation and Active Vibrations Control of Structures*. Istanbul, Turkey.

Kelly, J.M., and Konstantinidis, D.A. 2011. *Mechanics of Rubber Bearings for Seismic and Vibration Isolation*. *Mechanics of Rubber Bearings for Seismic and Vibration Isolation*. John Wiley & Sons, Inc.

Moon, B., Hang, G., and Kelly, J.M. 2002. "Design and Manufacturing of Fiber Reinforced Elastomeric Isolator for Seismic Isolation." *Journal of Materials Proccessing Technology* 130 (131): 145–50.

Osgooei, P.M., Tait, M.J., and Konstantinidis, D. 2017. Non-iterative computational model for fiber-reinforced elastomeric isolators. *Engineering Structures*, issued 2017.

Raaf, M.G.P. de, Tait, M.J., and Toopchi-Nezhad, H. 2011. "Stability of Fiber-Reinforced Elastomeric Bearings in an Unbonded Application." *Journal of Composite Materials* 45 (February): 1873–84.

Roeder, C.W., Stanton, J., and Feller, T. 1989. "Low Temperature Behaviour and Acceptance Criteria for Elastomeric Bridge Bearings." Washington, D.C., USA: Transportation Research Board.

Sciascetti, A.N., Al-anany, Y.M., and Tait, M.J. 2016. "The Effect of Temperature on the Lateral Response of Unbonded Fiber-Reinforced Elastomeric Isolators." In *Resilient Infrastructure*, 1–10. London.

Stevenson, A., and Maxwell, D.L. 1986. "Low Temperature Stiffening of Structural Rubber Bearings." In *International Rubber Conference*, 424–30. Goteborg, Sweden: The Swedish Institution of Rubber Technology.

Toopchi-Nezhad, H. 2014. "Horizontal Stiffness Solutions for Unbonded Fiber Reinforced Elastomeric Bearings." *Structural Engineering and Mechanics* 49 (3).

Toopchi-Nezhad, H., Drysdale, R.G., and Tait, M.J. 2009. "Parametric Study on the Response of Stable Unbonded-Fiber Reinforced Elastomeric Isolators (SU-FREIs)." *Journal of Composite Materials* 43 (15): 1569–87.

Toopchi-nezhad, H., Tait, M.J., and Drysdale, R.G. 2009. "Simplified Analysis of a Low-Rise Building Seismically Isolated with Stable Unbonded Fiber Reinforced Elastomeric Isolators Simplified Analysis of a Low-Rise Building Seismically Isolated with Stable Unbonded Fiber Reinforced Elastomeric Isolators." *Canadian Joural of Civil Engineering*.

Toopchi-Nezhad, H., Tait, M.J., and Drysdale, R.G. 2008a. "Lateral Response Evaluation of Fiber-Reinforced Neoprene Seismic Isolators Utilized in an Unbonded Application." *Journal of Structural Engineering* 134 (10): 1627–37.

Toopchi-Nezhad, H., Tait, M.J., and Drysdale, R.G. 2008b. "Testing and Modeling of Square Carbon Fiber-Reinforced Elastomeric Seismic Isolators." *Structural Control and Health Monitoring* 15: 876–900.

Van Engelen, N.C., Tait, M.J., and Konstantinidis, D. 2014a. "Model of the Shear Behavior of Unbonded Fiber-Reinforced Elastomeric Isolators." *Journal of Structural Engineering*, 1–11.

Van Engelen, N.C., Osgooei, P.M., Tait, M.J., and Konstantinidis, D. 2014b. "Experimental and Finite Element Study on the Compression Properties of Modified Rectangular Fiber-Reinforced Elastomeric Isolators." *Engineering Structures* 74. Elsevier Ltd: 52–64.

Yakut, A., and Yura, J. 2002. "Evaluation of Elastomeric Bearing Performance at Low Temperatures." *Journal of Structural Engineering* 128 (August): 995–1002.

Yang, Y., Chang, K., and Yau, J. 2003. "Base Isolation." In *Earthquake Engineering Handbook*, edited by Chen, W.F. New York: CRC Press.

Zayas, V.A., Low, S.S., and Mahin, S.A. 1990. "A Simple Pendulum Technique for Achieving Seismic Isolation." Earthquake Spectra.

CHAPTER 2

THE EFFECT OF TEMPERATURE ON THE LATERAL, VERTICAL AND ROTATIONAL RESPONSE OF UNBONDED FIBER-REINFORCED ELASTOMERIC ISOLATORS

2.1 INTRODUCTION

Fiber-reinforced elastomeric isolators (FREI) are a relatively recent development in the field of base isolation. They have been researched for their potential to be a lighter and less expensive alternative to current devices such as low-damping rubber, lead-plug rubber and high-damping rubber isolators. These traditional isolators are comprised of layers of rubber and rigid steel shims that provide the bearing with vertical stiffness. By replacing the steel shims with layers of fiber that have an elastic modulus similar to that of steel, studies indicate that FREI are able to satisfy vertical stiffness requirements for an isolator (Kelly 1999; Al-Anany et al. 2016). In addition, the use of fiber as reinforcement introduces flexibility into the isolator that affects its horizontal stiffness. However, it has been found that, compared to an equivalent steel reinforced elastomeric isolator (SREI), the decrease in flexural rigidity associated with FREI only results in a 10% reduction in lateral stiffness (Kelly 1999).

This reduced flexural rigidity allows FREI to exhibit unique and desirable properties at larger shear strains when employed in an unbonded application. Toopchi-Nezhad et al. (2008b) found that by selecting an isolator with an appropriate aspect

ratio (width to total height), unbonded FREI (U-FREI) develop a rollover mechanism that causes a reduction in effective lateral stiffness. The rollover mechanism begins to develop with a change in boundary conditions, as the horizontal faces of the isolator begin to lift off of the loading platens at low lateral displacements. Additional increases in displacement cause the lateral stiffness to decrease even further until the point of full rollover. This corresponds to a second change in boundary conditions that occurs at large lateral displacements. The faces of the isolator that were originally vertical at zero displacement roll over and come into full contact with the upper and lower loading platens, causing an increase in the effective lateral stiffness. This contact is significant as it prevents a negative lateral tangential stiffness from occurring (de Raaf et al. 2011). Van Engelen et al. (2014) performed a parametric study by varying the aspect ratio of U-FREI and found that a ratio below 2.5 causes instability in the rollover mechanism. Stability in FREI is defined as the isolator having a positive lateral tangential stiffness throughout its hysteresis loop and promotes re-centering capabilities during a seismic event (Toopchi-Nezhad et al. 2008a).

It has also been shown that the vertical and rotational response of U-FREI can achieve acceptable performance levels. Studies completed by Toopchi-Nezhad at al. (2008b, 2009) determined that U-FREI provide adequately high vertical stiffness and even outperform bonded FREI. In addition, after lateral cycling, the vertical stiffness was shown to not degrade by any significant measure. Similar studies were completed by Al-Anany and Tait to compare the vertical and rotational response of bonded and unbonded FREI (Al-Anany and Tait 2015, 2016). Numerical and experimental

investigations both found that the stress demand on the isolator was reduced when using U-FREI and as a result, large rotations could be accommodated. Al-Anany and Tait (2017a, 2017b) continued by determining the viability of U-FREI for bridge applications. It was shown that during cyclic rotations, similar to what would be induced by a bridge deck, U-FREI remained stable. Static rotations had negligible effect on the lateral response of U-FREI up to 0.03 radians, and typical lateral offsets expected of a bridge bearing did not significantly affect the vertical response of U-FREI.

2.1.1 Low Temperature Effects

The use of elastomeric bearings in bridges is common practice in North America and due to the cold, northern climates, bearings must be able to satisfy required performance levels at low temperatures. Early studies found that in general, low temperatures have a great influence on the properties of elastomers through crystallization and thermal stiffening (Russell 1951; Murray and Detenber 1961; Coe and Howgate 1986; Stevenson and Maxwell 1986). To examine the low temperature effects on elastomeric bridge bearings in more detail, Roeder et al. (1989) developed an extensive experimental program for the National Cooperative Highway Research Program (NCHRP). Lateral tests to 25% shear strain were conducted on elastomer specimens at a rate of 1% shear strain per second, or 100 seconds for a full cycle. The report confirmed that there are two main mechanisms that cause stiffening in elastomers. The first mechanism, called instantaneous thermal stiffening, is almost independent of time and solely a function of the ambient temperature. A decrease in

temperature results in a rapid increase in stiffness. In addition, the stiffness increase is amplified significantly once the temperature is below the second order transition temperature of the compound. This temperature, approximately -60 °C for natural rubber, marks the transition of an elastomer into a hard and brittle state that causes stiffness increases of more than 50 times room temperature values (Roeder et al. 1989). The second stiffening mechanism is called low temperature crystallization and is the result of nucleation and crystal growth processes that transition the elastomer structure into a semi-crystalline state (Bukhina and Kurlyand 2007). This process is not immediate and starts to occur after a delay from when the temperature is decreased, at which point the stiffness of the elastomer slowly increases over time. As the degree of crystallinity in the elastomer reaches equilibrium, crystallization slows and the increase in stiffness begins to plateau (Stevenson and Maxwell 1986). It was reported by both Murray and Detenber (1961) and Roeder et al. (1990) that natural rubber compounds are less affected by low temperature crystallization compared to neoprene and that the increase in stiffness was more gradual.

The results and some of the recommendations presented in the NCHRP report by Roeder et al. (1989) were adopted by AASHTO and are still included in the current Standard Specification for Plain and Laminated Elastomeric Bridge Bearings (AASHTO 2016). In this standard, elastomeric bearings can be categorized into one of five grades and must meet the required grade for their designated service location. The standard outlines various quasi-static tests that can be performed on the elastomer of a bearing to determine if a specified grade is met. For example, the elastomer of a grade

five bearing must have a stiffness of no more than four times its room temperature value after being conditioned for 28 days at -37 ± 2 °C. This is the strictest criteria for a bearing grade and is influenced by the maximum duration at which crystallization is still active, as recommended by Roeder et al. (1989). In the Canadian Highway Bridge Design Code (CHBDC 2014), bearings are not categorized. They must be conditioned for a minimum of 14 days at a temperature equal to the minimum mean daily temperature for the service location of the bearing.

These studies, as well as many others, have confirmed that elastomers can undergo large increases in stiffness at low temperatures (Kulak and Hughes 1993; Yakut et al. 2002; Fuller et al. 2004; Constantinou et al. 2007; Pinarbasi et al. 2007; Cardone and Gesualdi 2012; Sciascetti et al. 2016). This information presents a concern for engineers designing bridge bearings for cold climates. The shear forces that result from an increase in stiffness will be transferred to the bridge during a seismic event and must be limited to prevent damage. The objective of this paper is to evaluate the lateral, vertical and rotational response of unbonded, natural rubber FREI under the influence of varying low temperatures and conditioning durations.

2.2 TEST SPECIMENS

A total of seven FREI pads were manufactured in the Applied Dynamics Laboratory (ADL) at McMaster University. Each FREI contained seven layers of natural rubber, with a shear modulus of approximately 0.85 MPa and a durometer hardness of 55, and 6 layers of bi-directional carbon fiber cloth. The outer two layers of rubber were half the thickness of the internal layers. The natural rubber used in this

study is similar to a compound that has been previously used in commercially available steel reinforced elastomeric isolators. The pads were heated to activate the hot-vulcanization bonding agent used to fuse the layers together. Each pad was cut into four ¼ scale isolators having dimensions of 64 mm x 64 mm x 19 mm and a total thickness of rubber (t_r) of 18 mm. These dimensions provided each isolator with a shape factor of 5.52 and an aspect ratio of 3.37. The shape factor (the loaded area of one side divided by the perimeter load-free area of a single layer of rubber) influences vertical stiffness while the aspect ratio dictates stability.

Scaled specimens were used in this study due to the capacity of the test setup in the ADL. The properties of the scaled specimens at room temperature can be related to full-scale properties using dynamic similitude requirements (Harris and Sabnis 1999). To the best of the authors' knowledge, this has not been studied for low temperature testing. As a result, the findings presented herein are only representative of scaled specimens. The success of this study will indicate the need for additional future testing at larger scale or full-scale to be completed in order to fully evaluate the impact of potential scale effects.

FREI cut from the same pad were grouped together and designated for a specific test and conditioning duration as shown in Figure 2.1. This was done to ensure specimens of the same conditioning duration for each test could be accurately compared. Each FREI specimen was only used for a single test at a single temperature and the designations are found in Table 2.1. The temperatures chosen are taken from those given in AASHTO Standard Specification for Plain and Laminated Elastomeric

Bridge Bearings (AASHTO 2016). According to the standard, a Grade 1 bearing is tested at room temperature (RT). A FREI conditioned for 14 days at -18°C or -26°C corresponds to a Grade 2 or Grade 3 bearing, respectfully, and a FREI conditioned for 28 days at -37°C is a Grade 5 bearing.

2.3 TEST SETUP

The setup that was used throughout this study is depicted in Figure 2.2 and is capable of applying vertical and lateral displacements to the specimens, as well as rotations. This is possible through the use of three actuators that can be controlled individually. One actuator is attached horizontally to the loading beam to apply lateral displacements, while the other two actuators are attached vertically to opposite sides of the loading beam. These apply vertical loads and rotations independently of the horizontal actuator. In between the vertical actuators is a pedestal consisting of a large column section that transfers load to the base, and lower and upper platens that sandwich two 3-axis load cells. The specimens are placed within an insert that attaches to the upper platen and loading beam. This insert contains steel plates that have been roughened to have a coefficient of friction similar to that of concrete.

These roughened plates were cooled when being used during low temperature testing. It was found that the test specimen would experience a sudden increase in temperature when placed into the setup and would form a thin layer of water between the isolator and the plates. Pinarbasi et al. (2007) also experienced this and found that the water layer could cause or promote slip during testing. For this reason, blocks of dry ice were used to cool the plates to at least -15°C prior to each test. An added benefit

of using dry ice was that after sublimation, the carbon dioxide that was produced would displace the air within the chamber. This effectively created an environment with zero humidity that prevented moisture in the air from freezing to the plates. To maintain this environment, a conditioning chamber consisting of acrylic sheets was constructed around the roughened plates. The loading beam was free to move laterally, and the chamber expanded and contracted to allow vertical loading and rotations.

Each low temperature FREI specimen was conditioned within a monitored freezer that maintained the required temperature to within 2°C. Once the plates were cooled to the target temperature, one specimen was removed from the freezer and placed within the setup. The test commenced immediately and took less than 60 seconds for the lateral and vertical tests, and 100 seconds for the rotational tests.

2.4 TESTING PROCEDURES

The goal of this testing was to obtain the hysteresis loops and from these, calculate the effective stiffness and energy dissipation of each FREI specimen. The following tests will be used to demonstrate the acceptable performance of the U-FREI specimens at low temperatures.

2.4.1 Lateral Testing

Dynamic lateral tests were conducted under a constant vertical pressure of 7 MPa that was applied using a ramp function. Pressure was calculated as the load applied from the two vertical actuators, divided by the area of the isolator specimen. A vertical pressure of 7 MPa was chosen as it represents the serviceability limit state

under all loading conditions and the ultimate limit state under permanent loading conditions in Ontario Provincial Standard Specification 1202, Material Specification for Bearings – Elastomeric Plain and Steel Laminated (OPSS 2016).

For low temperature testing, the CHBDC recommends lateral testing at three displacement amplitudes equal to 0.2, 0.4 and 0.6 times the design displacement of a prototype isolator (CHBDC 2014). In order to capture the behaviour of U-FREI exhibiting rollover, the specimens were instead laterally displaced at five lateral amplitudes equalling a ratio of the total thickness of rubber (t_r) in the FREI. The amplitudes were 0.25, 0.50, 0.75, 1.00, and 1.50 of t_r, as given in Figure 2.3. These lateral displacement amplitudes were chosen in order to represent the expected displacements imposed on both a bearing (non-seismic loading) and an isolator (seismic loading) (CHBDC 2014). The displacements were each applied as three, fully reversed, sinusoidal cycles at the rate of 76mm per second. This rate is consistent with the rate previously used by others (Al-Anany 2017a).

The resultant data was processed to calculate the stiffness and energy dissipation of each cycle. The effective lateral stiffness is given in Equation (2.1) and calculated by taking the slope of a line that connects the point of maximum lateral load and displacement with the point of minimum lateral load and displacement (ASCE 2013).

$$K_{L,eff} = (F_{L,max} - F_{L,min})/(\Delta_{L,max} - \Delta_{L,min}) \quad (2.1)$$

The variables $F_{L,max}$, $F_{L,min}$, $\Delta_{L,max}$, and $\Delta_{L,min}$ are the maximum and minimum values of lateral load and maximum and minimum values of lateral displacement, respectively. The corresponding energy dissipation for each cycle, E_D, was determined by calculating the area enclosed by the hysteresis loop formed for each cycle.

In order to aid in analysis, the effective equivalent viscous damping ratio, ζ, was also calculated. It is given as (CHBDC 2014):

$$\zeta = \frac{E_D}{2\pi K_{L,eff}\Delta_{avg}^2} \qquad where \qquad \Delta_{avg} = \frac{\Delta_{L,max} + |\Delta_{L,min}|}{2} \tag{2.2}$$

2.4.2 Vertical Testing

All vertical tests were completed under load control, where each specimen was monotonically loaded up to 7 MPa and subjected to three, fully reversed, sinusoidal cycles as recommended by ISO-22762 (ISO 2010). The time history of the test is given in Figure 2.4. Each cycle had an amplitude of ±20% of the load corresponding to 7 MPa.

The effective vertical stiffness of each cycle was calculated using the same formula as the lateral tests. It is given in Equation (2.3) and is updated to indicate that the force and deflections are in the vertical direction. The energy dissipation of each cycle was also calculated.

$$K_{v,eff} = (F_{v,max} - F_{v,min})/(\Delta_{v,max} - \Delta_{v,min}) \tag{2.3}$$

2.4.3 Rotational Testing

The rotational tests were all conducted by first monotonically loading each specimen to 7 MPa. The two vertical actuators used a feedback loop to apply the rotations to the specimen at a rate of 0.004 radians per second. In the AASHTO LRFD standard (2012), the maximum service limit rotation for steel reinforced elastomeric bearings is the total of rotations from service loads and a 0.005 radian allowance for uncertainties. To determine U-FREI rotational behaviour for different maximum service limits, two, fully reversed sinusoidal cycles were completed for each rotation of 0.005, 0.01, 0.02 and 0.03 radians and are shown in Figure 2.5.

Similar to the lateral and vertical tests, the effective rotational stiffness of each specimen was calculated. It was found by taking the slope of the line that connects the point of maximum moment and rotation with the point of minimum moment and rotation, as given in Equation (2.4):

$$K_{\theta,eff} = (M_{max} - M_{min})/(\theta_{max} - \theta_{min}) \quad (2.4)$$

Where, M_{max}, M_{min}, θ_{max}, and θ_{min} are the maximum and minimum values of moment and maximum and minimum values of rotation, respectfully. Energy dissipation, E_D, was calculated using the area enclosed by the hysteresis loop at each cycle.

2.4.4 Scragged Properties

The reason that multiple full cycles were completed at each amplitude for the lateral, vertical and rotational tests is that the bearings stabilize after their initial cycles.

Both Van Engelen et al. (2014a) and Al-Anany et al. (2015) found that the hysteresis loops became consistent and stable at each amplitude, such that the effective lateral stiffness and energy dissipation values at the second and third cycles converge. This is shown in Figure 2.6 where it can be seen that the second and third hysteresis loops are similar, indicating that the loops have stabilized for the current displacement amplitude and scragged properties have been achieved. This was also shown by Sciascetti et al. (2016) to occur at low temperature for lateral tests.

At room temperature, the lateral and vertical tests required three cycles to stabilize, while it was found for the rotational tests that there was negligible difference between the second and third hysteresis loops, allowing for only two cycles to be completed. The reduction in cycles for the rotational tests also enabled the length of each test to be closer to that of the lateral and vertical tests. This allowed testing to progress with as little affect as possible from the external environment on the low temperature specimens. Throughout this paper, the scragged properties of the FREI specimens will be referred to and used to illustrate comparisons.

2.5 LATERAL RESPONSE

2.5.1 Specimen Hysteresis Loops

The U-FREI specimens were tested according to the procedures described in Section 2.4.1. The scragged hysteresis loops of the room temperature specimens from each of the 1 and 14 Day tests have been plotted in grey against the low temperature specimens from the same conditioning duration in Figure 2.7. The lateral forces, F, have been normalized by the shear modulus, G, and the isolator area, A and the lateral

displacements, u, have been normalized by the total thickness of rubber in the isolator, t_r. A video recording was taken of each test in order to confirm that slip did not occur. Upon review, it was determined that slip occurred in two specimens: during the final lateral displacement cycles for the 14 Day | -18°C specimen and during the cycles of 0.50, 0.75 and 1.00 t_r for the 28 Day | -37°C specimen. The hysteresis loop has been omitted for the first case, as the amount of slip was large, while the hysteresis loops for the second case were kept, as the amount of slip was minimal. The peak load values of these three hysteresis loops are expected to be higher since slip indicates the maximum force was not attained. This would result in larger effective stiffness values, but due to the small amount of slip, the values are not expected to be greatly different than those recorded. For this specimen, a reduction in the roughness of the plates may have contributed to slip, as it was the last specimen to be tested. These hysteresis loops have been included in Figure 2.7, but are distinguished as a dashed line.

Prior to the lateral testing, there were several concerns regarding the response of the U-FREI specimens at low temperatures. It was postulated that delamination might occur between the fiber and rubber layers during rollover or that the rollover mechanism would not be as effective. In general, each specimen was found to exhibit acceptable rollover behaviour at all displacement amplitudes and no delamination was found to have occurred in any specimen. Beginning with the room temperature specimens, the difference between the 1 Day and 14 Day FREI is negligible. Examining individual low temperature U-FREI, it can be seen in the hysteresis loops that the peak force reached by each, using the room temperature specimen for reference (grey line),

increases as the temperature is decreased. This indicates the expected effect that instantaneous thermal stiffening should have is present. The individual loops at smaller displacements can be seen to grow wider and have rotated such that with the same displacement a larger load is achieved, which indicates an increase in stiffness. The wider loops indicate an increase in the energy dissipation associated with each U-FREI at low temperature.

For the -18°C and -26°C specimens, the difference in the hysteresis loops is hard to distinguish between the 1 Day and 14 Day tests. This lack of differences indicates that with 14 days of conditioning at these two low temperatures, crystallization is not present in the specimens. If it were, an increase in load at each displacement amplitude would be expected, as well as much wider loops as a result of increased energy dissipation.

In comparison, the U-FREI conditioned at -37°C illustrate the effect of crystallization on the hysteretic behaviour. Each hysteresis loop at the lowest three displacement amplitudes is shown to become more rotated (increased stiffness) as the conditioning duration is increased from 1 through 28 days. At 28 days, the change in the hysteresis loops is significant and the peak load at each displacement amplitude is nearly twice as large as the previous conditioning durations. The area within the hysteresis loops is much larger as well. The observed differences in the hysteretic response of these specimens clearly indicate that the effect of crystallization is present. From this information, it can be concluded that the temperature that results in the largest rate of crystallization is below -26°C and is postulated to be near -37°C. Past

studies indicate that for natural rubber, the rate of maximum crystallization has been observed as being between -25°C and -35°C, which is in agreement with the results presented here. (Murray and Detenber 1961; Yura et al. 2001; Roeder et al. 1989).

2.5.2 Effective Lateral Stiffness

From the hysteresis loops presented in Figure 2.7, the values for effective stiffness and energy dissipation were calculated. This allows for a more accurate comparison of what occurred at each lateral displacement amplitude for each hysteresis loop. In Figure 2.8, the effective lateral stiffness is presented for each low temperature specimen. The values at each displacement have been normalized by the corresponding values obtained from the specimen tested at room temperature. The grey dashed line indicates that slip occurred at those points.

The 1 Day test specimens, highlighted with triangular markers, illustrate the almost immediate effect that low temperatures have on bearings. By reducing the temperature of the FREI to -37°C, the maximum stiffness increase is more than two times the room temperature value. As with the hysteresis loops, Figure 2.8 shows little difference between the 1 and 14 Day specimens at -18°C and -26°C. The 1 Day curves of each temperature are overlapped by the 14 Day curves, again indicating that crystallization at these temperatures does not affect stiffness.

The -37°C specimens clearly show the effect that long duration conditioning can have on FREI and most other bearings as well. As the conditioning duration is increased from 1 to 14 to 28 days, the stiffness increases substantially. At low lateral

displacements, the largest increase in stiffness is more than six times the room temperature values. At this temperature, crystallization has a large effect on the performance of FREI. It can be seen that the change in stiffness decreases with an increase in displacement by a much larger factor, the longer it has been conditioned. The stiffness of the 1 Day specimen dropped at most by 0.5 times the room temperature values between 0.25 and 1.5 t_r. (i.e. 2.1 to 1.6 for the 1 Day | -37°C specimen), While the 28 Day specimen dropped from a 6.1 times stiffness increase at a displacement of 0.25 t_r, to a 2.7 times stiffness increase at 1.50 t_r.

This phenomenon can be explained by the reorientation of the molecular structure of an elastomer at low temperature. Crystallization causes elastomers to transform into a semi-crystalline state through nucleation and crystal growth processes. The crystals that grew as a result, must now be fractured in order to accommodate the required displacements. Once fractured at low displacements, they are not able to contribute as much to shear resistance at larger displacements. As a result, the lateral stiffness at larger displacements decreases. With a higher degree of crystallization in the specimen due to a longer conditioning duration, the increase in stiffness that will be observed is larger, as seen with the 28 Day specimen.

According to the AASHTO Standard Specification for Plain and Laminated Elastomeric Bridge Bearings (2016), the increase in stiffness allowed after low temperature conditioning is a maximum increase in stiffness of four times the room temperature value. This limit is in reference to stiffness values obtained from quasi-static testing, but can be extended to the dynamic lateral tests completed in this study.

The 28 Day | -37°C specimen, at lateral displacements of 0.25 – 0.75 t_r, does not pass this criterion, indicating that according to AASHTO, it may not be appropriate to be used as a Grade 5 bearing.

2.5.3 Lateral Energy Dissipation

The energy dissipation values of each FREI are presented in Figure 2.9, in the same format as was done for effective stiffness. It can be seen that the trends for energy dissipation are quite similar to those from effective stiffness. At 1 day of conditioning, the specimens show an increase in energy dissipation with a decrease in temperature. This increase is greatest at the lowest displacement and is twice that at room temperature for -18°C, and four times for -37°C. When compared to the increases in stiffness at this displacement, the increase in energy dissipation is twice as large. This continues when analyzing the 14 Day | -37°C specimen. The increase in stiffness is by three, while the energy dissipation increases by a factor of six. This trend stops at the 28 Day specimen, as crystallization may have a larger effect on stiffness at this duration, than it does energy dissipation. The other 14 Day specimens confirm that crystallization of the elastomer has not started to occur yet and can be seen from the similarities between the 1 Day and 14 Day curves.

The downward sloping curves illustrate that the increase in energy dissipation at larger amplitude cycles is less. This change is again much larger for the specimens that exhibited the effects of crystallization. At lower displacements, the crystals that formed must be fractured and as a result, much more energy is dissipated. As the displacements increase, the crystals that have already been broken cannot dissipate

additional amounts of energy, resulting in a decrease in energy dissipation. The 28 Day specimen does not follow this trend, but there was some slip that occurred at those displacements. More energy may have been dissipated as a result of abrasion against the loading supports.

2.5.4 Effective Damping Ratio

In order to aid in analysis of the lateral specimens, the effective equivalent viscous damping ratio was calculated and is given in Figure 2.10. From Equation 2.4, it is shown that the damping ratio is dependent on the effective stiffness and the amount of energy dissipated. In this study, the displacement amplitudes were constant for all specimens and do not affect the damping ratio calculation as temperature and conditioning duration are varied.

The damping ratio can be seen to increase with a decrease in temperature after a single day of conditioning. Following 14 days of conditioning at the same three temperatures, the damping ratio is shown to remain a near constant value. The increase in damping ratio after a single day is due to a larger increase in energy dissipation than stiffness. After 14 days of conditioning, the change in stiffness is approximately the same as the increase in energy dissipation, resulting in similar damping ratios. For the specimen conditioned for 28 days, the damping ratio decreases at the lowest displacement amplitude due to crystallization, when compared to the specimens conditioned for 1 and 14 days at the same temperature. At this displacement of 0.25 t_r, the effective stiffness increased significantly more than the increase in energy dissipation, causing the observed decrease in damping. Overall, the damping values,

excluding those values corresponding with slip, are quite similar, ranging from 1.4 to 2.3 times the room temperature values. In addition, the change in damping ratio between the low temperature and room temperature specimens is shown to be consistent across all displacement amplitudes.

2.6 VERTICAL RESPONSE

2.6.1 Specimen Hysteresis Loops

The room temperature FREI specimens were the first to be tested according to the procedure outlined in Section 2.4.2. These hysteresis loops have been plotted in grey in Figure 2.11. The room temperature specimens, when compared, are quite similar to one another, as was seen with the lateral, room temperature hysteresis loops. The low temperature tests have been plotted over top of the room temperature specimens for comparison. They have been plotted from when the cycles commenced, to when the cycles finished. The starting point corresponding to 7 MPa was taken to be zero strain. This was done to allow more accurate visual comparisons between specimens.

Unlike the lateral testing, the vertical tests were only carried out for three cycles around an average pressure of 7 MPa and as a result, the hysteresis loops in Figure 2.11 have been shown in full. Examining individual specimens, it can be seen that each FREI has some degree of offset between cycles, where subsequent loops are shifted towards positive vertical strain. This is commonly exhibited with FREI as they settle under compressive forces, but does not alter the effective vertical stiffness calculated from the loops (Van Engelen et al. 2014; Al-Anany et al. 2015). As the temperature is

decreased and the conditioning duration lengthens, the drifting decreases, confirming that it is affected by the stiffness of the FREI. A larger compressive load would be required to cause this to occur with stiffer FREI.

Similar to the lateral tests, the 1 Day specimens are shown to increase in stiffness as temperature is decreased. The low temperature loops in black do not reach the same vertical strain values as the room temperature specimen results in grey. At each low temperature, an increase in stiffness can be seen by comparing the 1 Day and 14 Day hysteresis loops. The angle of rotation of each set of loops can be seen to increase with respect to the horizontal axis. At much larger rotations, an increase in stiffness is associated with the 28 Day | -37°C specimen. These trends almost mirror those of the lateral tests, indicating that the effect of instantaneous thermal stiffening and crystallization also influence the vertical response of FREI. The specimens will be examined more closely by comparing the effective vertical stiffness and energy dissipation.

2.6.2 Effective Vertical Stiffness

In order to calculate the effective vertical stiffness, the third cycle of the hysteresis loops presented above were used. The curves for effective stiffness normalized by the stiffness value at room temperature are given in Figure 2.12 as a function of temperature. The solid curve gives the effect of temperature after 1 day of conditioning. A decrease in temperature correlates with an increase in vertical stiffness, but the increase is not significant; only a maximum increase of 20% over the room temperature specimen. The same trend exists for the 14 Day specimens marked by the

dashed line. The difference between the two curves at the temperatures of -18°C and -26°C is insignificant, but at -37°C the stiffness increases by one and a half times. For the 28 Day | -37°C specimen, the stiffness increase is just over 1.8 times the room temperature value. This indicates that crystallization does have as significant effect on the vertical stiffness of FREI as the lateral stiffness, but in order to determine its significance of this stiffness increase, the vertical frequency of the conditioned FREI was analyzed. The equation to calculate vertical frequency is given by:

$$f_v = 1/(2\pi) * \left(K_{v,eff} g/(PA)\right)^{1/2} \quad (2.5)$$

where g is the gravitational constant, P is the constant pressure applied (7 MPa) and A is the area of the one loaded face of the FREI. Completing the calculation for the 28 Day | -37°C specimen results in a 35% increase in vertical frequency when compared to the room temperature specimen. This result is potentially beneficial as the vertical frequency must be large enough to prevent rocking motions at the bridge deck level. An increase in frequency can aid in accomplishing this.

2.6.3 Vertical Energy Dissipation

The amount of energy an isolator dissipates vertically controls the length of time induced rocking or vertical motions will last. Adequate energy dissipation is required as these motions are unwanted in the system. The amount of energy dissipated by each specimen has been plotted as a function of time for multiple conditioning durations in Figure 2.13. The 1 Day curve shows a small, general increase in dissipated energy across all temperatures, which corresponds with the minimal change in stiffness

found in Figure 2.12. Again, instantaneous thermal stiffening has a negligible effect on the vertical response of U-FREI. The 14 Day curve exhibits a similar trend to what was found from the lateral tests; crystallization does not affect FREI at -18°C and -26°C. Conversely, with the 14 Day | -37°C specimen, the amount of energy dissipated is less than the room temperature value. The decrease is amplified even larger for the 28 Day | -37°C specimen, with the energy dissipation found to be only half the room temperature value. This is the opposite of what would be expected using the lateral energy dissipation data as a reference.

This reduction, however, is postulated to have occurred because of the testing procedure. The vertical tests were completed under load control, and were consistently cycled to predefined pressures, 7 MPa ± 20%. With a stiffer isolator, the vertical strain required to achieve these loads is decreased. Even though crystals have formed in the elastomer due to crystallization, they are not broken during testing because the isolator does not need to accommodate large vertical deflections. As a result, crystallization does not provide added energy dissipation when tested under load control. If displacement control had been used and the specimens were cycled at set displacement amplitudes, it is expected that the energy dissipation of the low temperature FREI would have increased. In addition, the increase in stiffness of the FREI at low temperature reduces the amount that the isolator bulges horizontally. At room temperature, this bulging would cause tension in the carbon fiber reinforcement. An increase in energy dissipation would occur due to rearrangement and slip caused by frictional forces among individual fiber strands (Kelly 1999).

Although a decrease in energy dissipation is not desirable, the accompanied increase in vertical stiffness and frequency at low temperature reduces the significance of requiring the isolator to dissipate energy against vertical motion.

2.7 ROTATIONAL RESPONSE

2.7.1 Specimen Hysteresis Loops

Each U-FREI specimen designated for rotational testing was subjected to the testing procedures given in Section 2.4.3. The hysteresis loops are provided in Figure 2.14 in the same format as the loops presented for the lateral and vertical responses. The moment, M, has been normalized by the product of the shear modulus, G, the isolator area, A, and the total thickness of rubber in the isolator, t_r. The room temperature loops are plotted in grey along with the low temperature loops for comparison. The observed trends are very similar to those from the lateral response with respect to the effect of instantaneous thermal stiffening on the 1 Day specimens, and the effect of crystallization on the U-FREI conditioned for 14 and 28 days. For the 1 Day specimens, a decrease in temperature caused an increase in stiffness, which is shown by counter-clockwise rotation of the loops away from the horizontal axis. In comparing the 1 Day specimens to the corresponding 14 Day specimens at the same conditioning temperatures of -18°C and -26°C, there is shown to be small differences. A much larger change is noticeable when comparing the three -37°C specimens. At small rotations, the stiffness increases and the area within the hysteresis loops reduces, indicating a decrease in energy dissipation. It can be slightly seen in the 14 Day | -37°C specimen that the loops that started as oval, become more curved and follow an 'S'

shape. This is even more prominent with the 28 day | -37°C specimen, where the 'S' shape is clearly visible.

The reason for this change in shape is due to the FREI specimens being unbonded to the loading supports. At room temperature, it was found that with low vertical pressure a lift-off mechanism would form causing a softening behaviour in the bearing under larger rotations (Al-Anany and Tait 2015). During lift-off, depicted in Figure 2.15, the boundary conditions change as the upper loading support lifts off from the surface of the FREI, such that the loaded area gradually reduces as rotation is increased. Lift-off was previously restricted in bridge design codes, but is no longer (AASHTO 2012). It has been shown to be beneficial in reducing strain, as well as limiting rotation that could cause delamination, when compared to bonded isolators (Al-Anany and Tait 2015). This softening behaviour is shown to be exhibited by the low temperature specimens and is explained below by the increase in effective rotational stiffness with a decrease in temperature.

2.7.2 Effective Rotational Stiffness

The rotational tests included only two full cycles at each of the four rotations specified, unlike the lateral and vertical tests. As mentioned previously, similar scragged values were obtained from the second and third cycles during preliminary rotational tests. The effective stiffness as a result was calculated for the second cycle at each displacement for the FREI specimens. The results are provided in Figure 2.16, in the same format as the lateral tests.

In general, except for the 14 and 28 Day | -37°C specimens, the increase in rotational stiffness at each amplitude is quite consistent, with a slight parabolic nature to the curves. Examining the 1 Day specimens, it can be observed that there is a small increase in stiffness as temperature is decreased. The 14 day specimens, at temperatures higher than -37°C, do not differ much from their 1 Day equivalents. As was found for the lateral and vertical tests, U-FREI are not affected by crystallization at these temperatures. The 14 and 28 Day | -37°C specimens are where the benefit of using unbonded FREI can be seen. The increase in stiffness due to crystallization for these specimens is up to 2.4 times the room temperature values, but reduces at larger rotations. This is due to the softening behaviour that arises from the lift-off mechanism present in U-FREI. Since the test was completed under displacement control, which more closely mimics the rotation of a bridge deck girder, the rotation that is applied must be reached. As the isolator becomes stiffer, the resistance to this rotation is increased and a larger moment is applied in order to reach the required rotation. With a bonded isolator, this may have caused delamination between the rubber and reinforcing layers from the large increase in internal forces. However, because of the ability of unbonded FREI to exhibit lift-off, this does not occur and the specimens remained damage free.

2.7.3 Rotational Energy Dissipation

The amount of energy dissipated by the FREI specimens at each rotation is given in Figure 2.17. It can be observed that the FREI behave similarly to one another, despite the different conditioning durations and temperatures. The maximum increase

in rotational energy dissipated is just under 1.30 times the room temperature value. The 1 Day test specimens show an increase in energy dissipation between the -18°C and -37°C specimens, but the 1 Day | -26°C is an outlier in this case. The same is true of the 14 Day specimens. The -26°C FREI, again does not follow the trend, but is still quite close as the difference in the increase compared to room temperature is small.

The specimen conditioned for 28 days at -37°C does not fit into any trends previously described. There is actually a large decrease in the amount of energy dissipated when compared to the 14 Day specimen at the same temperature. This is postulated to be in part due to crystallization and the lift-off mechanism that occurs for a specimen of increased stiffness. At low rotations, the strain in the isolator may not be large enough to break any crystals that had formed in the elastomer over the additional 14 conditioning days when compared to the 14 Day | -37°C specimen. As rotations increase, the loaded area of the isolator decreases with increased lift-off, but the strain in the loaded portion continues to increase in order to accommodate the rotations. Crystals in the elastomer can now be fractured at the larger strain values, but since the volume of elastomer under strain is decreased, there are less crystals to break and the energy dissipated does not rise as high as one might expect.

2.8 SUMMARY AND CONCLUSIONS

The purpose of this study was to investigate the lateral, vertical and rotational behaviour of unbonded fiber-reinforced elastomeric isolators (U-FREI) subjected to low temperatures, for application to bridges located in cold, northern climates. In total, 28 U-FREI were conditioned for durations of 1 to 28 days at temperatures of -18°C to

-37°C before being tested. The 1 day testing duration was used to determine the effect of instantaneous thermal stiffening at different temperatures on the response of U-FREI, while the testing duration of 14 days was used to determine the effect of low temperature crystallization. A 28 day test duration was included for the temperature of -37°C in order to match the requirements for a Grade 5 low temperature bearing from the AASHTO Standard Specification for Plain and Laminated Elastomeric Bridge Bearings (AASHTO 2016). Laterally, one third of the specimens were subjected to dynamic cyclic loading up to a lateral displacement amplitude of 1.50 times the total height of rubber in the isolator. The vertical response was tested in accordance to ISO-22762 for the next third and the final third of specimens were subjected to rotations up to 0.03 radians. The results that were observed from these tests are summarized into three sections.

Lateral Response

It was found that instantaneous thermal stiffening had a large effect on effective stiffness and dissipated energy for the lateral specimens. As the temperature was decreased, the specimens stiffened and dissipated larger amounts of energy. The damping ratio was shown to increase with the decrease in temperature due to a larger increase in energy dissipation than stiffness. The most severe case of -37°C caused approximately a two-times increase in effective stiffness and a four-times increase in energy dissipation.

The tests conducted under longer conditioning durations showed that crystallization did not affect the isolator specimens at -18°C and -26°C. Values after

14 days were similar to those after a single day of conditioning. However, at -37°C, as the conditioning duration was increased, the stiffness and energy dissipation of the isolators greatly increased. The increase for both at 14 days was of a comparable magnitude, as the damping ratio remained similar to the corresponding 1 day value. Following 28 days of conditioning, crystallization was found to have a greater effect on stiffness than it does on the isolators ability to dissipate energy. The former tripled compared to the 1 day value, while the latter only doubled. As a result, the damping ratio was shown to decrease.

The increase in damping ratio compared to the room temperature specimen was also shown to remain constant across all displacement amplitudes. This indicates that the ratio between the increase in energy dissipation and the increase in effective stiffness is a constant regardless of the temperature.

Lastly, all specimens, except the U-FREI conditioned for 28 days at -37°C passed the criterion in AASHTO Standard Specification for Plain and Laminated Elastomeric Bridge Bearings specifying that the increase in stiffness must be less than four-times the room temperature value.

Vertical Response

In general, all U-FREI provided acceptable behaviour in response to cyclic vertical testing at all conditioning temperatures and durations. The effects of low temperatures caused a moderate increase in stiffness that correlates to an increase in the vertical frequency of the isolator. This is beneficial, as the vertical frequency must be sufficiently high to prevent rocking motions.

It was observed that all specimens conditioned for 1 day, and the -18°C and -26°C specimens at 14 days exhibited similar values of stiffness and energy dissipation. The stiffness increase was approximately 20%, while the energy dissipation remained approximately the same as the room temperature values. For the specimens conditioned at -37°C for 14 and 28 days, the amount of energy dissipated decreased by up to half the room temperature values. The significance of this is reduced due to the accompanied increase in vertical frequency.

Rotational Response

During the cyclic rotation tests, the use of FREI in the unbonded application allowed all specimens to remain undamaged throughout testing. The study determined that the rotational stiffness response to low temperature followed the same trends as the lateral tests. A decrease in temperature caused an increase in stiffness, while an increase in conditioning duration resulted in little change when compared to the values obtained from 1 day of conditioning for the temperatures of -18°C and -26°C. The stiffness increase was similar regardless of the amplitude of the cyclic rotations.

The -37°C specimens conditioned for 14 and 28 days developed a larger increase in stiffness. In addition, as the angle of rotation increased, the specimens exhibited lift-off and a softening behaviour formed, resulting in a lower stiffness at the larger rotations. In regards to the amount of energy dissipated by the specimens, all values were approximately the same. The largest increase was 30% with the largest decrease only 10% of the room temperature values.

Using this data, further studies will be investigated to numerically determine the effectiveness of U-FREI when employed as the isolation system for a bridge located in a cold, northern climate. The lateral response of a bridge conditioned for 28 days at -37°C will be of interest to determine the validity of the criterion preventing U-FREI from being used as a Grade 5 bearing. Overall, but limited to the findings presented in this paper, the experimental results indicate that performance of U-FREI laterally, vertically and rotationally is acceptable under the effects of low temperatures.

2.9 REFERENCES

AASHTO. 2012. "LRFD Bridge Design Specifications." Washington, D.C.: American Association of State Highway and Transportation Officials.

AASHTO. 2016. "M 251-06 Standard Specification for Plain and Laminated Elastomeric Bridge Bearings." Washington, D.C.: American Association of State Highway and Transportation Officials.

Al-Anany, Y.M., Van Engelen, N.C., and Tait, M.J. 2015. "Vertical and Lateral Behavior of Unbonded Fiber-Reinforced Elastomeric Isolators." *Journal of Composite Structures*, no. 1: 1–11.

Al-Anany, Y.M., Van Engelen, N.C., and Tait, M.J. 2016. "An Experimental Investigation on the Vertical and Lateral Behaviour of Unbonded Fiber-Reinforced Elastomeric Isolators." *Composites for Construction, under Review*.

Al-Anany, Y.M., and Tait, M.J. 2015. "A Numerical Study on the Compressive and Rotational Behaviour of Fiber Reinforced Elastomeric Isolators (FREI)." *Composite Structures* 133. Elsevier Ltd: 1249–66.

Al-Anany, Y.M., and Tait, M.J. 2016. "An Experimental Study of the Vertical and Rotational Behaviour of Unbonded Fiber- Reinforced Elastomeric Isolators (U-FREI) for Bridge Applications,." *Composites Part B: Engineering*.

Al-Anany, Y.M., and Tait, M.J. 2017a. "Experimental Assessment of Utilizing Fiber Reinforced Elastomeric Isolators as Bearings for Bridge Applications." *Composites Part B: Engineering* 114 (1): 373–85.

Al-Anany, Y.M., and Tait, M.J. 2017b. "Fiber Reinforced Elastomeric Isolators for the Seismic Isolation of Bridges." *Composite Structures* 160. Elsevier Ltd: 300–311.

ASCE. 2013. *ASCE/SEI 7-10: Minimum Design Loads for Buildings and Other Structures*. New York, USA: American Society of Civil Engineers.

Bukhina, M.F., and Kurlyand, S.K. 2007. *New Concepts in Polymer Science: Low-Temperature Behaviour of Elastomers*. Boca Raton: CRC Press.

Cardone, D., and Gesualdi, G. 2012. "Experimental Evaluation of the Mechanical Behavior of Elastomeric Materials for Seismic Applications at Different Air Temperatures." *International Journal of Mechanical Sciences* 64 (1): 127–43.

Coe, D.G., and Howgate, P.G. 1986. "Effect on Crystallization of Low Frequency Shear Strain." In *International Rubber Conference*. Goteborg, Sweden: The Swedish Institution of Rubber Technology.

Constantinou, M.C., Whittaker, A.S., Kalpakidis, Y., Fenz, D.M., and Warn, G.P. 2007. "Performance of Seismic Isolation Hardware under Service and Seismic Loading." MCEER-07-0012. Buffalo, NY. Multidisciplinary Center for Earthquake Engineering Research.

CAN/CSA-S6. 2014. "Canadian Highway Bridge Design Code (CHBDC)." Ontario: Canadian Standard Association.

Fuller, K.N.G., Gough, J., and Thomas, A.G. 2004. "The Effect of Low-Temperature Crystallization on the Mechanical Behavior of Rubber." *Journal of Polymer Science, Part B: Polymer Physics* 42 (11 SPEC. ISS.): 2181–90.

Harris, H.G., and Sabnis, G.M. 1999. *Structural modeling and experimental techniques.* CRC Press, New York.

ISO. 2010. *Elastomeric Seismic-Protection Isolators*. ISO 22762-. Geneva, Switzerland: International Organization for Standardization.

Kelly, J.M. 1999. "Analysis of Fiber-Reinforced Elastomeric Isolators." *Journal of Seismology and Earthquake Engineering* 2 (1): 19–34.

Kulak, R.F., and Hughes, T.H. 1993. "Frequency and Temperature Dependence of High Damping Elastomers." Oak Ridge, TN, USA: Office of Scientific and Technical Information.

Murray, R.M., and Detenber, J.D. 1961. "First and Second Order Transitions in Neoprene." *Rubber Chemistry and Technology* 34 (2): 668–85.

OPSS. 2016. *OPSS.MUNI 1202 Material Specification for Bearings - Elastomeric Plain and Steel Laminated.* Ontario Provincial Standards.

Pinarbasi, S., Akyuz, U., and Ozdemir, G. 2007. "An Experimental Study On Low Temperature Behavior Of Elastomeric Bridge Bearings." In *10th World Conference on Seismic Isolation, Energy Dissipation and Active Vibrations Control of Structures*. Istanbul, Turkey.

Raaf, M.G.P. de, Tait, M.J., and Toopchi-Nezhad, H. 2011. "Stability of Fiber-Reinforced Elastomeric Bearings in an Unbonded Application." *Journal of Composite Materials* 45 (February): 1873–84.

Roeder, C.W., Stanton, J., and Feller, T. 1989. "Low Temperature Behaviour and Acceptance Criteria for Elastomeric Bridge Bearings." Washington, D.C., USA: Transportation Research Board.

Russell, E.W. 1951. "The Crystallization of Vulcanized Natural Rubber at Low Temperatures." *Trans. Faraday Soc.* 47: 539.

Sciascetti, A.N., Al-Anany, Y.M., and Tait, M.J. 2016. "The Effect of Temperature on the Lateral Response of Unbonded Fiber-Reinforced Elastomeric Isolators." In *Resilient Infrastructure*, 1–10. London.

Stevenson, A., and Maxwell, D.L. 1986. "Low Temperature Stiffening of Structural Rubber Bearings." In *International Rubber Conference*, 424–30. Goteborg, Sweden: The Swedish Institution of Rubber Technology.

Toopchi-Nezhad, H., Drysdale, R.G., and Tait, M.J. 2009. "Parametric Study on the Response of Stable Unbonded-Fiber Reinforced Elastomeric Isolators (SU-FREIs)." *Journal of Composite Materials* 43 (15): 1569–87.

Toopchi-Nezhad, H., Tait, M.J., and Drysdale, R.G. 2008a. "Lateral Response Evaluation of Fiber-Reinforced Neoprene Seismic Isolators Utilized in an Unbonded Application." *Journal of Structural Engineering* 134 (10): 1627–37.

Toopchi-Nezhad, H., Tait, M.J., and Drysdale, R.G. 2008b. "Testing and Modeling of Square Carbon Fiber-Reinforced Elastomeric Seismic Isolators." *Structural Control and Health Monitoring* 15: 876–900.

Van Engelen, N.C., Tait, M.J., and Konstantinidis, D. 2014a. "Model of the Shear Behavior of Unbonded Fiber-Reinforced Elastomeric Isolators." *Journal of Structural Engineering*, 1–11.

Van Engelen, N.C., Osgooei, P.M., Tait, M.J., and Konstantinidis, D. 2014b. "Experimental and Finite Element Study on the Compression Properties of Modified Rectangular Fiber-Reinforced Elastomeric Isolators." *Engineering Structures* 74. Elsevier Ltd: 52–64.

Yakut, A. and Yura, J.A. 2002. "Parameters Influencing Performance of Elastomeric Bearings at Low Temperatures." *Journal of Structural Engineering* 128 (8): 986–94.

Yura, J., Kumar, A., Yakut, A., Topkaya, C., Becker, E., and Collingwood, J. 2001. "Elastomeric Bridge Bearings : Recommended Test Methods." Austin, TX, USA: Transportation Research Board.

Table 2.1: FREI pad designation.

Test	Pad	Duration (Days)	Temperature (°C)
Lateral	1	1	RT, -18, -26, -37
	2	14	
Vertical	3	1	
	4	14	
Rotational	5	1	
	6	14	
All Tests	7	28	-37

Figure 2.1: Photograph of U-FREI test specimens.

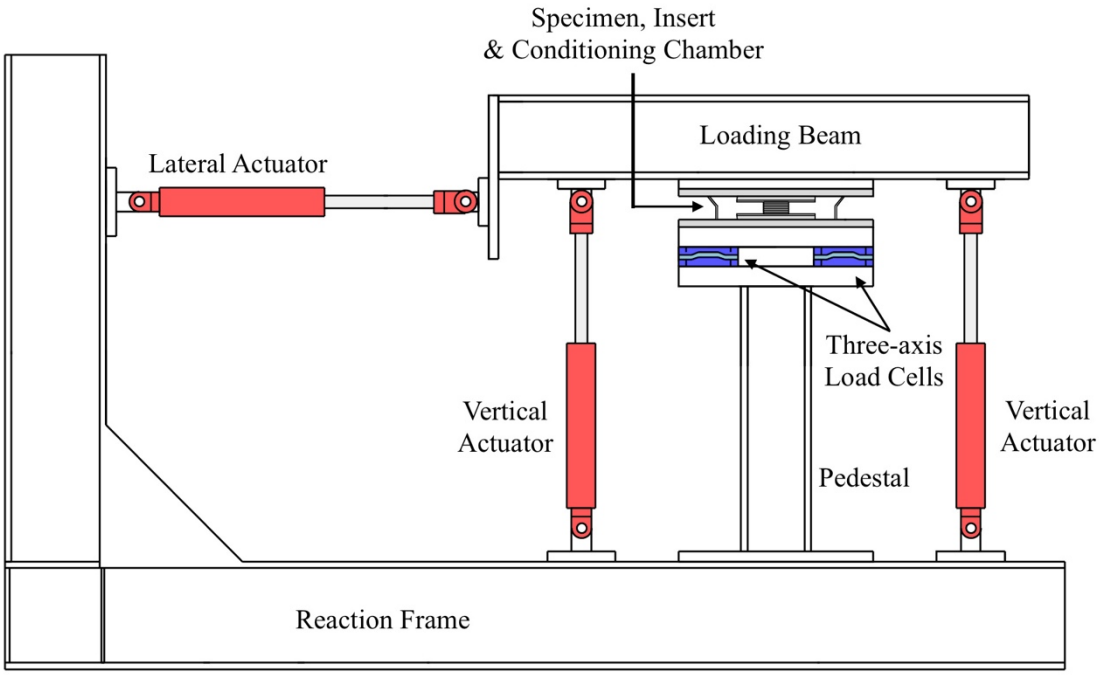

Figure 2.2: Three degree of freedom test setup.

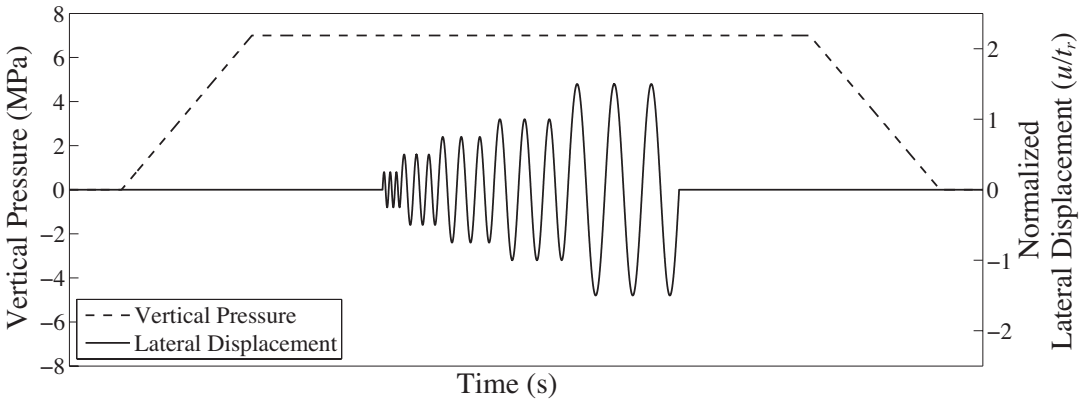

Figure 2.3: Vertical loading and lateral displacement time history for all lateral tests.

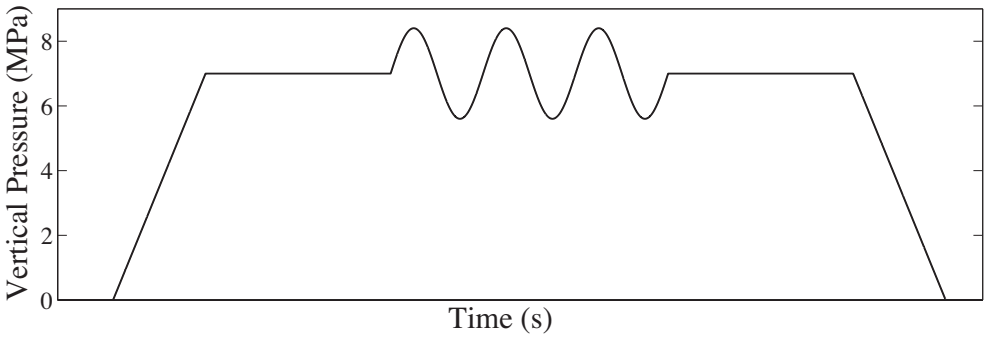

Figure 2.4: Vertical loading time history for all vertical tests.

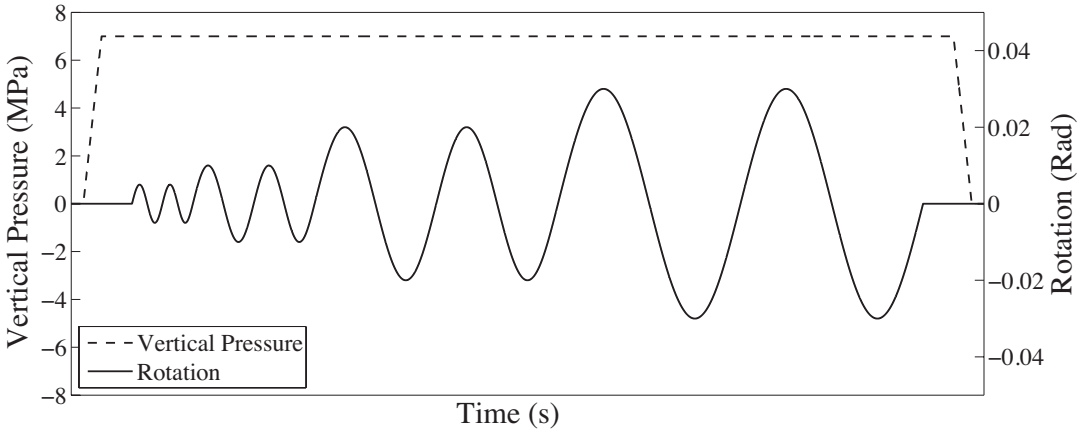

Figure 2.5: Vertical loading and rotation time history for all rotation tests.

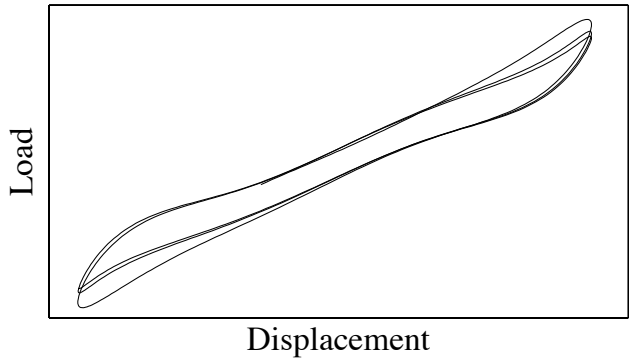

Figure 2.6: Example hysteresis loops to depict scragging.

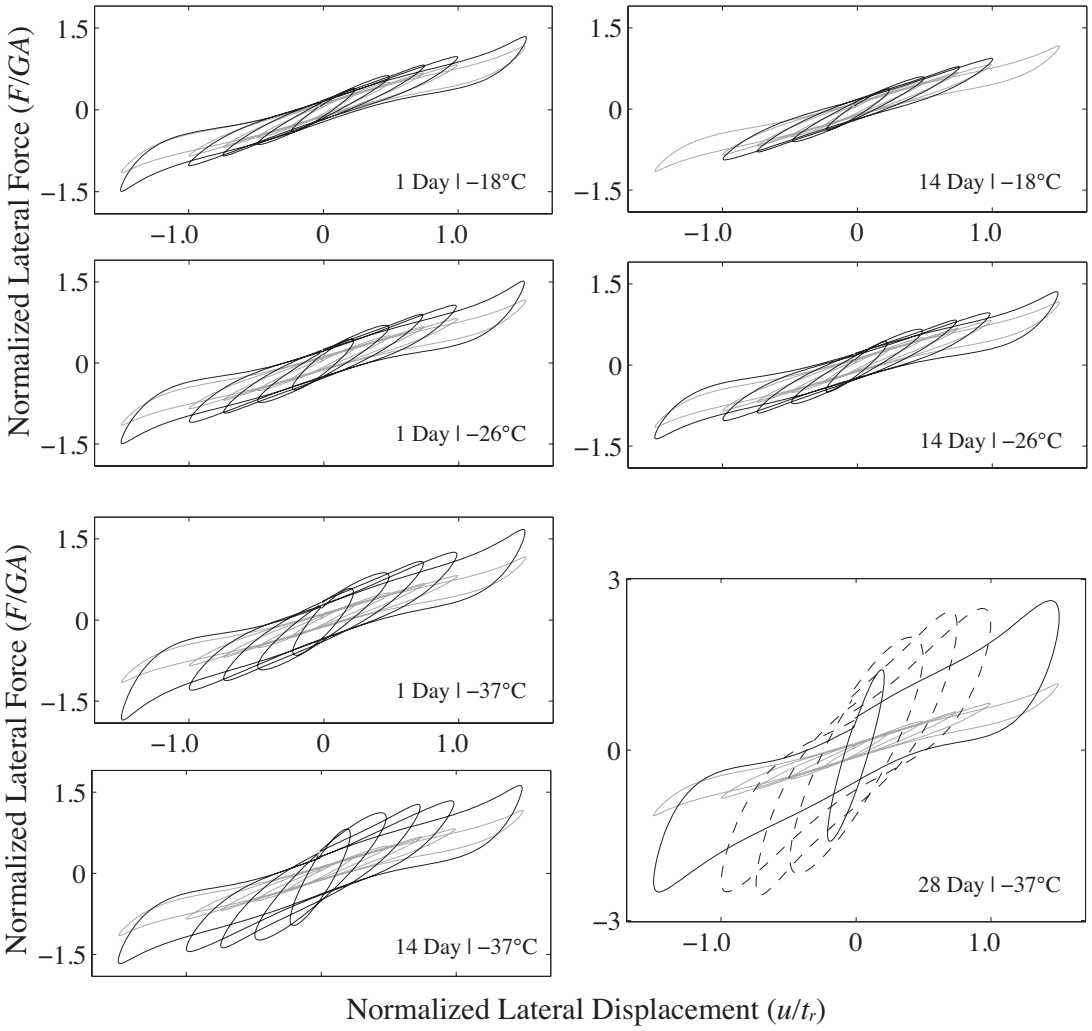

Figure 2.7: Normalized lateral response scragged hysteresis loop comparison of low temperature (black) to room temperature (grey) U-FREI specimens.

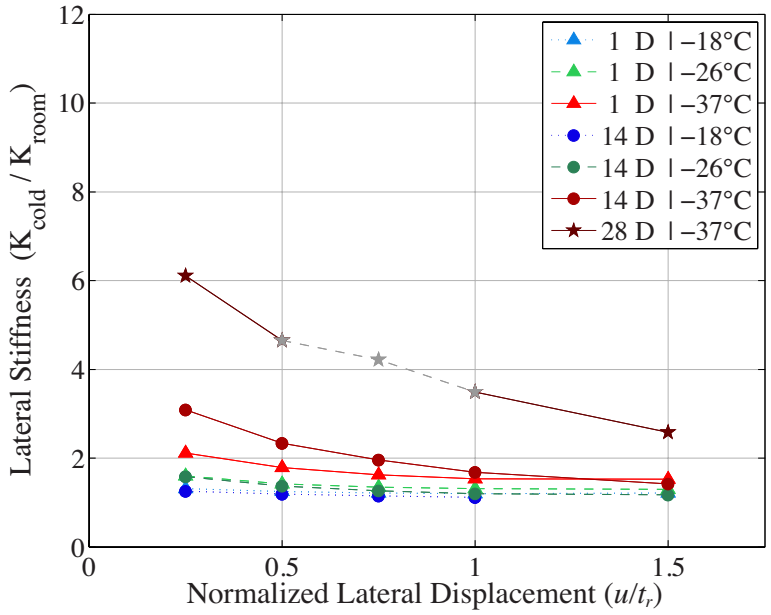

Figure 2.8: The effect of low temperature on lateral effective stiffness normalized against room temperature values.

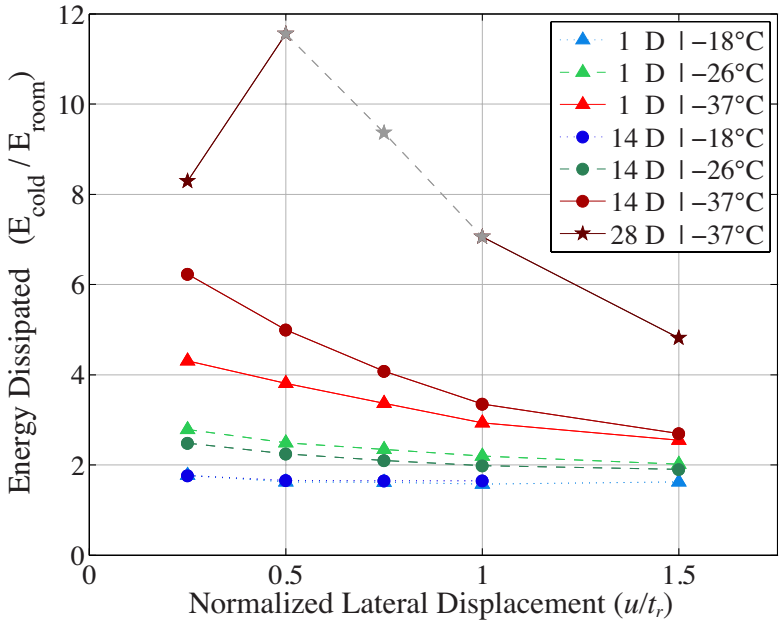

Figure 2.9: The effect of low temperature on lateral energy dissipation values normalized against room temperature.

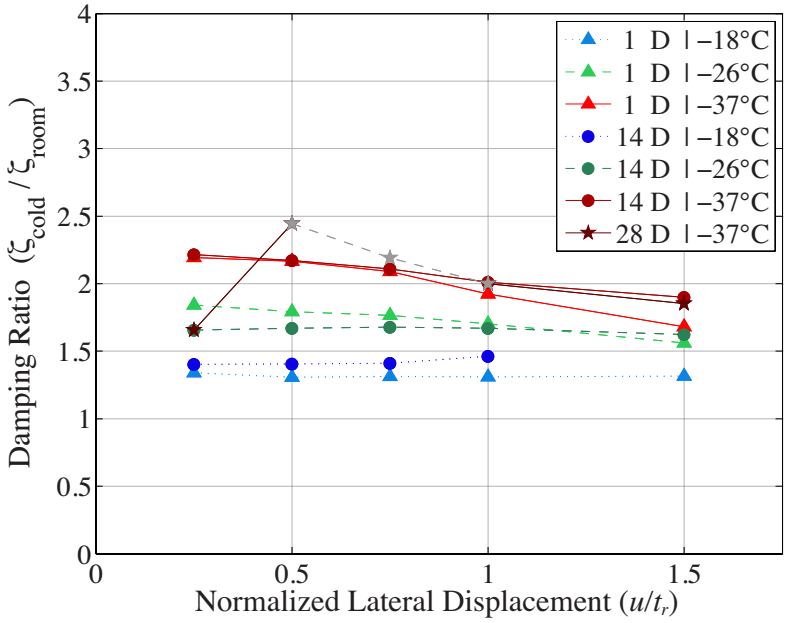

Figure 2.10: The effect of low temperature on effective damping ratio normalized against room temperature.

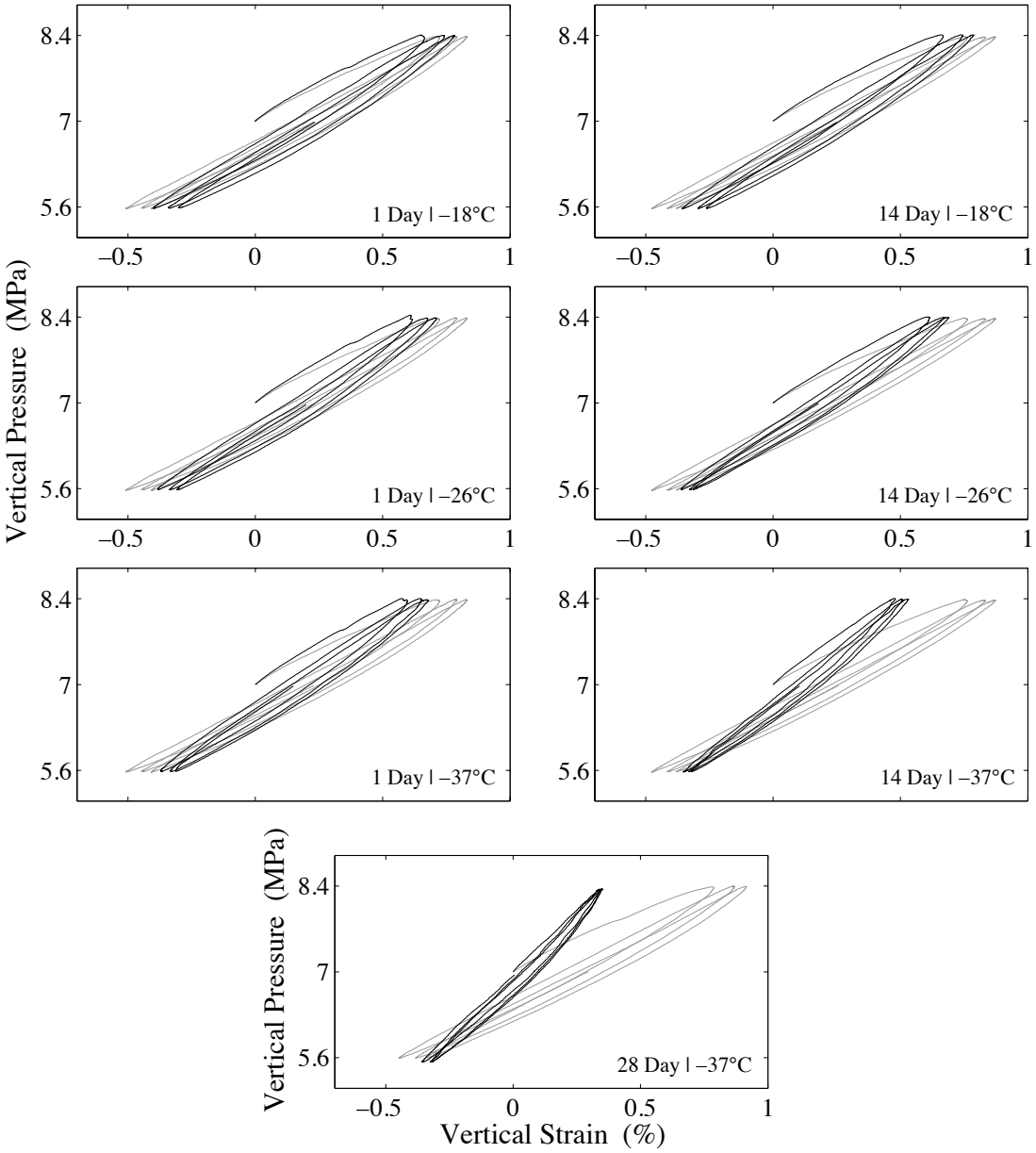

Figure 2.11: Vertical response hysteresis loop comparison of low temperature (black) to room temperature (grey) FREI specimens.

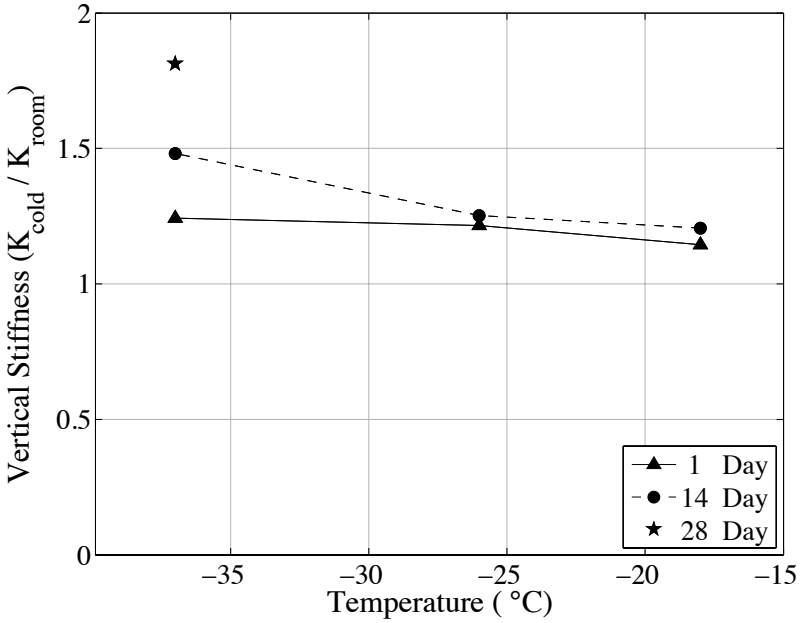

Figure 2.12: The effect of low temperature on vertical effective stiffness normalized against room temperature values.

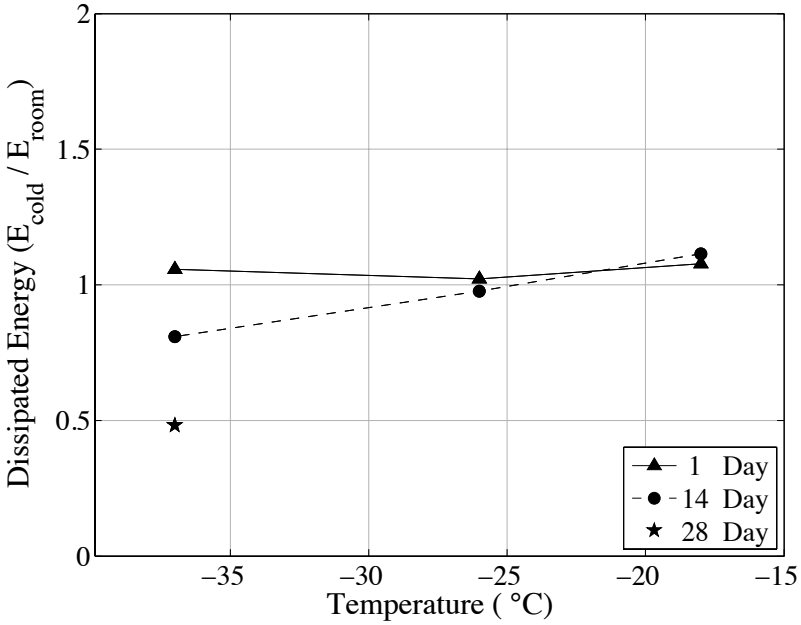

Figure 2.13: The effect of low temperature on vertical energy dissipation values normalized against room temperature.

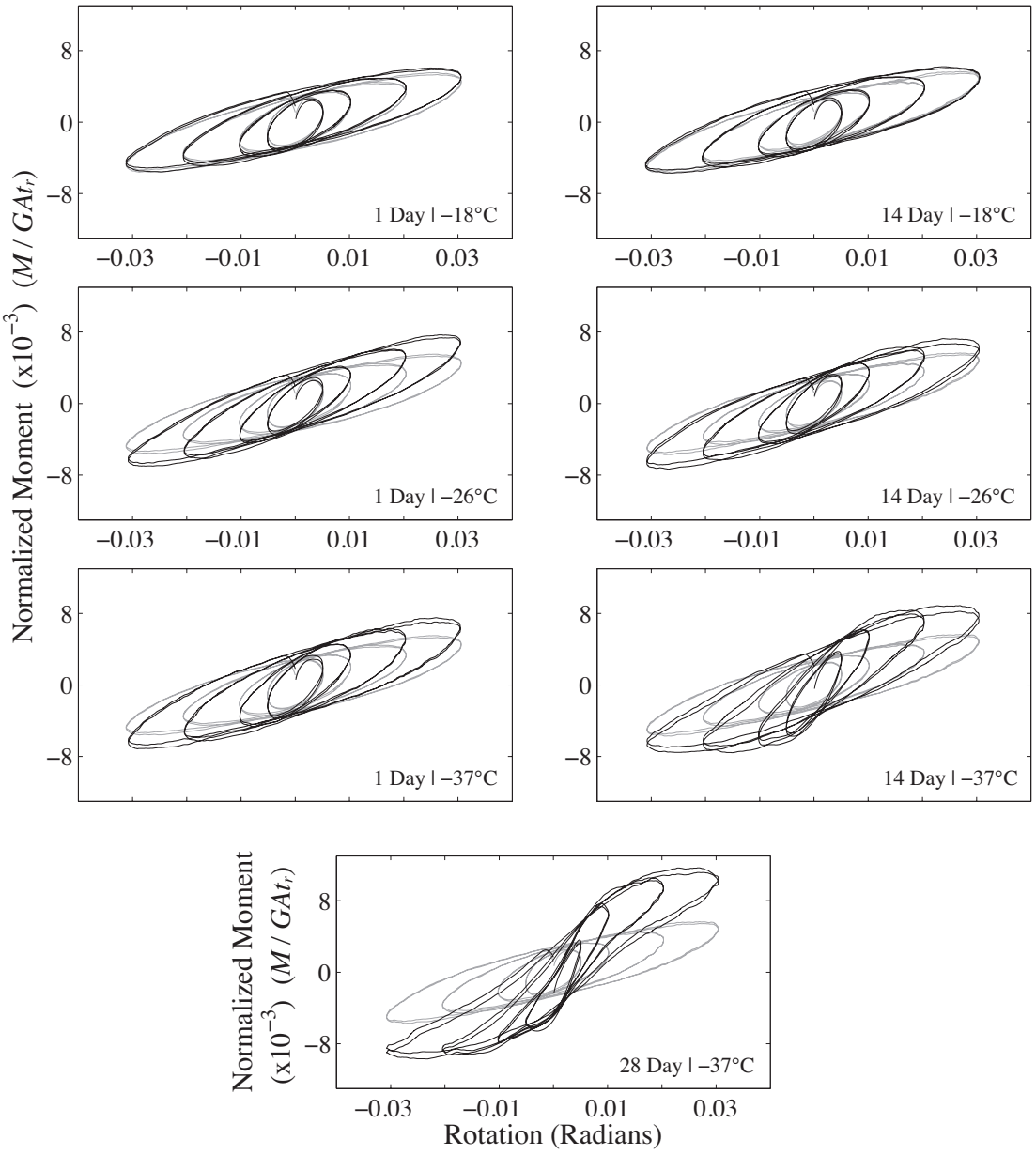

Figure 2.14: Rotational response hysteresis loop comparison of low temperature (black) to room temperature (grey) FREI specimens.

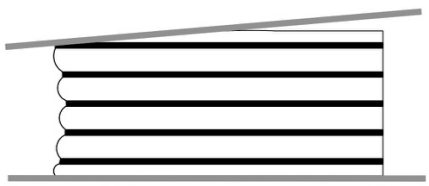

Figure 2.15: Lift-off in an unbonded-FREI.

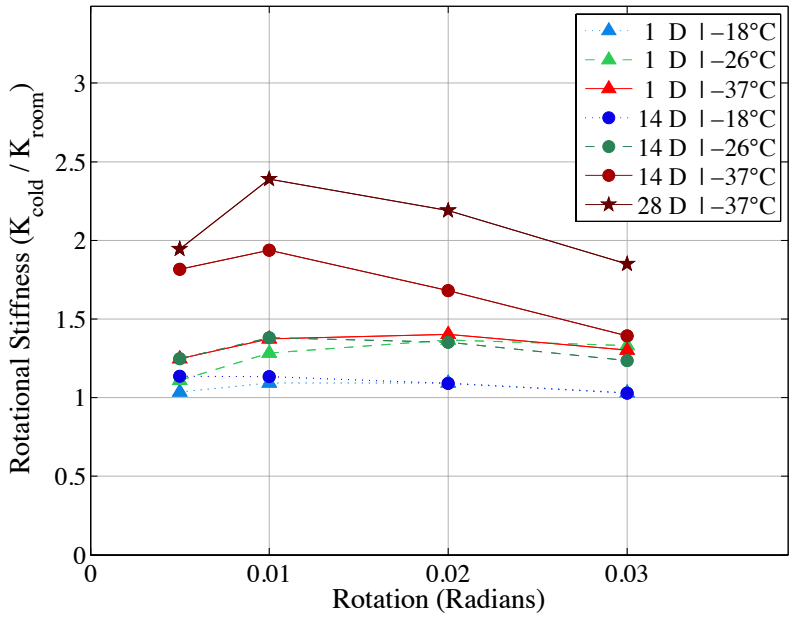

Figure 2.16: The effect of low temperature on rotational effective stiffness normalized against room temperature values.

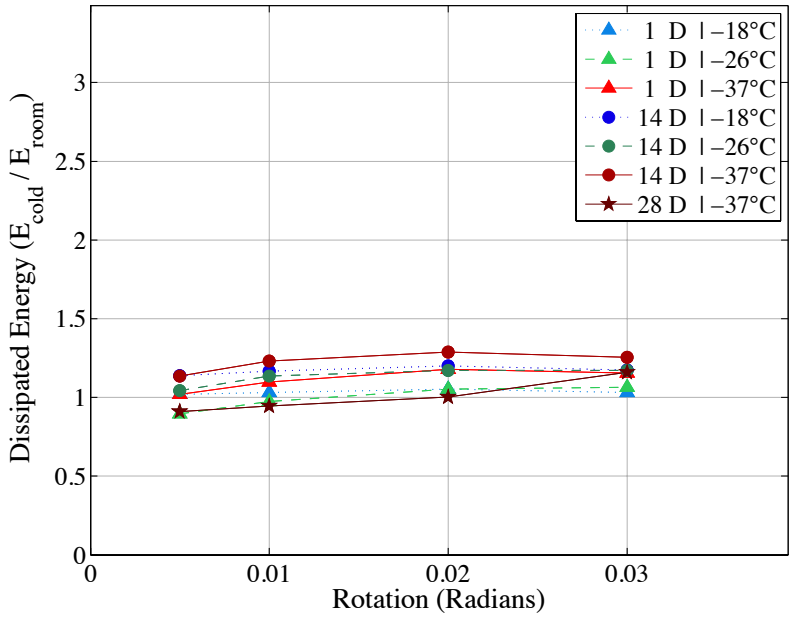

Figure 2.17: The effect of low temperature on rotational energy dissipation values normalized against room temperature.

CHAPTER 3

THE EFFECT OF TEMPERATURE ON THE SEISMIC PERFORMANCE OF A STRUCTURE ISOLATED WITH UNBONDED FIBER-REINFORCED ELASTOMERIC ISOLATORS

3.1 INTRODUCTION

It has been widely documented that base isolation can be employed to reduce the adverse effects that earthquakes have on structures. The placement of isolators beneath a structure at locations where load is transferred, essentially allows the structure to be separated from the foundation. This effectively uncouples the motion of the ground during a seismic event from the structure. Isolated structures are not just limited to being buildings; the seismic isolation of bridges has become much more common (Buckle et al. 2006). Isolators are used as a replacement to the typical bridge bearings that are located between the bridge deck and pier. The lower stiffness of the isolators compared to the piers allows movement of the deck during a seismic event to be accommodated by the isolator instead of by deformation in the piers. The reduction in stiffness also causes an increase in the period of the bridge, away from the predominant periods of ground motions. This reduces the acceleration of the bridge deck and as a result, base shear forces are smaller, limiting or completely avoiding damage to the piers.

The effectiveness of seismically isolating bridge structures has been detailed and promoted by many studies. Ghobarah and Ali (1988) and Jangid (2004) found through numerical modeling that the introduction of lead-rubber isolators could greatly reduce deck accelerations and base shear forces in the bridge piers. Wang et al. (1998) and Jangid (2008) determined that friction-pendulum isolators also provide effective seismic isolation of bridge structures. Buckle et al. (2006) developed a manual titled *Seismic Isolation of Highway Bridges*, which gives an overview of design principles and the analysis of isolators to promote the application of seismic isolation to highway bridges. It was determined that there were more than 200 bridges isolated in North America at the time of writing. These include the Golden Gate Bridge in San Francisco and the AirTrain Light Rail System servicing JFK International Airport in New York. In Canada, six bridges in Vancouver, including the Lions Gate Bridge, are seismically isolated, along with a pedestrian bridge near Ottawa that transverses King's Highway 417. Of all the bridges isolated in North America, 75% were isolated with lead-plug rubber isolators as of 2006 (Buckle et al. 2006). Buckle et al. (2011) also developed a document titled *Seismic Isolation Design Examples of Highway Bridges*. It allows the design process to be better understood by presenting design examples that highlighted the application of seismic isolation to highway bridges considering various types of isolation devices.

More recently, research has been completed on the use of fiber-reinforced elastomeric isolators (FREI) in bridge applications (Al-Anany and Tait 2017a; Al-Anany and Tait 2017b). FREI utilize layers of carbon-fiber cloth as a replacement for

the rigid steel shims that are typical of elastomeric bearings. They can be placed unbonded (U-FREI) between the bridge deck and piers or abutments to provide effective isolation during a seismic event. Toopchi-Nezhad et al. (2008) found that the increase in flexibility of the FREI, as a result of the use of carbon fiber, allows a rollover mechanism to develop in this unbonded application. Figure 3.1 depicts that as the lateral displacement amplitude is increased, the horizontal faces of the U-FREI begin to lift off of the upper and lower loading platens, which results in a decrease in effective stiffness. With large lateral displacements, full rollover begins to occur, where the initially vertical faces of the U-FREI become horizontal and in full contact with the loading platens. This contact causes a hardening behaviour to occur and acts to limit the maximum lateral displacement of the isolator.

A significant amount of research has been completed on FREI, detailing different lateral, vertical and rotational behaviours of the isolators (Toopchi-Nezhad et al. 2009; de Raaf et al. 2011; Van Engelen et al. 2014; Al-Anany et al. 2015; Al-Anany et al. 2016). With respect to the vertical response, it was shown that U-FREI provide sufficiently high vertical stiffness that does not significantly degrade following lateral cyclic loading (Toopchi-Nezhad et al. 2009). The response of U-FREI under rotation was studied by Al-Anany and Tait (2016) and was determined that U-FREI can be subjected to much larger rotations than bonded FREI. The stress demand is greatly reduced in the unbonded isolators due to the upper loading support's ability to *lift-off* during rotation (see Figure 2.15). Further studies indicate that rotations up to 0.03

radians have a negligible effect on the lateral behaviour of U-FREI (Al-Anany et al. 2017b).

All of these studies were completed at room temperature, but the response of FREI at low temperatures is important, especially in northern climates. To be used with bridges, the FREI must be able to provide acceptable performance while subject to the same low temperatures that the bridge itself will experience. A major effect of low temperature on elastomers has been widely documented to cause elastomers to exhibit an increase in stiffness in response to a reduction in temperature (Murrey et al. 1961, Stevenson et al. 1986, Roeder et al. 1990, Yakut and Yura 2002, Sciascetti et al. 2016). This stiffness increase can be separated into two mechanisms that affect the performance of elastomeric isolators such as FREI. The first mechanism is called instantaneous thermal stiffening and corresponds to the elastomer transitioning into a brittle, glassy state. (Roeder et al. 1989). This provides a rapid change in stiffness in response to a change in temperature. As the glass transition temperature is approached (approximately -65°C for natural rubber), the stiffness increase can be greater than 50 times the room temperature value (Roeder et al. 1989). Low temperature crystallization is the second mechanism and can cause stiffness increases over the span of weeks after the initial incubation period where no stiffness increase is observed. The change in stiffness is a result of the transition of the structure of the rubber into a crystalline state through nucleation and crystal-growth processes (Bukhina and Kurlyand 2007). The effect of these two mechanisms on the behaviour of U-FREI was studied by Sciascetti and Tait (2016; 2017). It was found that U-FREI exhibited acceptable behaviour in

most instances as defined by the AASHTO Standard Specification for Plain and Laminated Elastomeric Bridge Bearings (2016).

In this study, an existing numerical model of U-FREI lateral behavior is updated using the lateral experimental results presented by Sciascetti and Tait (2017) in order to account for the effects of low temperatures. The updated model is then used to evaluate the lateral seismic performance of a three-span bridge structure isolated with U-FREI at multiple conditioning temperatures and durations. It will be shown that a bridge structure isolated with U-FREI can provide reasonable performance at low temperatures.

3.2 EXPERIMENTAL RESULTS SUMMARY

The experimental research program completed by Sciascetti and Tait (2017) was carried out to determine how the previously mentioned low temperature stiffening mechanisms affect the response of unbonded-FREI to lateral, vertical and rotational testing. The isolators were tested under multiple temperatures and conditioning periods, as per the AASHTO Standard Specification for Plain and Laminated Elastomeric Bridge Bearings (2006). In total, 28, ¼ scale isolators were constructed in the Applied Dynamics Laboratory at McMaster University, with eight constructed for the purpose of lateral displacement tests. Each isolator had physical dimensions of 64 mm in both length and width, and a total height of rubber (t_r) of 18 mm. This resulted in a shape factor of 5.52 and an aspect ratio of 3.37. The shape factor controls the compression modulus of the bearing and is the ratio of the loaded area of a single elastomer layer to the unloaded or perimeter area. The aspect ratio controls the stability

of the isolator and is the ratio of the width to total height of the isolator. The shear modulus of the rubber was found experimentally to be 0.86 MPa. The FREI were conditioned in a freezer that maintained the desired temperature within two degrees Celsius. The temperatures studied were room temperature, -18°C, -26°C and -37°C, at conditioning periods of 1 and 14 days. A conditioning period of 28 days was also studied for -37°C as suggested by Roeder at al. (1989) and AASHTO (2006) due to low temperature crystallization.

The results of the lateral testing indicated that at all temperatures, the U-FREI were able to maintain a positive lateral tangential stiffness throughout the hysteresis loops at all displacement amplitudes, satisfying the requirement in Canadian Highway Bridge Design Code (CHBDC 2014). All U-FREI, except the specimen conditioned at -37°C for 28 days, passed the criteria in AASHTO (2016) requiring a maximum increase in stiffness of four times the room temperature value. This study successfully showed the ability of U-FREI to be used at low temperatures.

3.3 ISOLATOR MODEL

Several models have been constructed to simulate the lateral response of U-FREI. The earliest model proposed by Toopchi-Nezhad et al. (2008) consisted of 11 parameters that were used to describe the restoring and damping force of the bearing in an iterative approach. Two new models were subsequently proposed; Model 1 was based on the amplitude and rate of the lateral response and Model 2 was a bilinear model that considered stiffness and damping to be rate independent (Toopchi-Nezhad et al. 2009). With Model 2, only three parameters are required to model the behaviour

of the U-FREI. The response predicted by the model was in better agreement with experimental responses than the previously proposed models. Love et al. (2011) modified a linearized Bouc-Wen model with a fifth-order polynomial in order to simulate the lateral softening and stiffening response of U-FREI. The limitation of these models is that they still require an iterative analysis procedure in order to achieve convergence as different parameters correspond to hysteresis loops at different displacement amplitudes. Further details on the algorithm used to implement the iterative analysis procedure is presented by Toopchi-Nezhad et al. (2009). The Pivot-Elastic model, developed by Osgooei et al. (2017) addressed this limitation. It is non-iterative and is calibrated using the values of effective stiffness and damping taken from experimental tests, instead of being fit to an entire set of hysteresis loops. The model consists of a bilinear pivot hysteresis model placed in parallel with a non-linear elastic model in order to capture the change in effective stiffness present at larger displacement amplitudes. It was found that the Pivot-Elastic model predicted experimental shake table results better than the previous iterative models proposed by Toopchi-Nezhad et al. (2009).

3.3.1 Current Model

Al-Anany et al. (2017) built off of the Pivot-Elastic model to develop the Takeda-Elastic model. This non-iterative, rate-independent model consists of a non-linear elastic spring and a hysteretic element that are applied in parallel to provide the lateral response of U-FREI under varying displacement amplitudes, while allowing for

a more practical implementation in OpenSees. A visual representation of the model is provided in Figure 3.3.

The hysteretic element is the Takeda bilinear plastic model (Takeda et al. 1970), which is used to add energy dissipation into the isolator model. It requires three parameters to define the bilinear behaviour; the initial stiffness k_1, the yield displacement u_y and the post-yield stiffness k_2. In comparison, the pivot hysteretic model used by Osgooei et al. (2017) contains five extra parameters that can be employed to modify degradation in the loops. One limitation of the Takeda model is that when the lateral displacement is less than the yield displacement, there is no energy dissipation in the system. The force, as a function of the lateral displacement of the isolator "u", is described by the model as follows:

$$\begin{aligned} F_{Takeda}(u) &= k_1 u && u < u_y \\ F_{Takeda}(u) &= k_1 u_y + k_2(u - u_y) && u \geq u_y \end{aligned} \tag{3.1}$$

The non-linear elastic spring element is used to capture the varying stiffness of U-FREI at different displacement amplitudes. This lateral behaviour can be classified as having three phases as depicted in Figure 3.1. The first phase occurs at smaller displacement amplitudes when the horizontal faces of the U-FREI have not yet lifted from the supports causing a linear elastic behaviour. The second phase introduces a softening behaviour where the effective stiffness of the isolator degrades due to the onset of the rollover mechanism. This occurs at moderate lateral displacement amplitudes and corresponds with the horizontal faces gradually lifting from the

supports. At large displacement amplitudes, the initially vertical faces make contact with the supports causing a subsequent increase in effective stiffness.

In order to accurately describe the aforementioned lateral forces, a fifth order polynomial is used to model the force-displacement curve of the non-linear elastic spring. This portion of the model does not include any energy dissipation. The spring force can be expressed as a function of the lateral displacement of the isolator and is given by:

$$F_{Spring}(u) = a_1 u + a_3 u^3 + a_5 u^5 \tag{3.2}$$

where a_1 through a_5 are unique model parameters that are fit to experimental data. Parameters a_2 and a_4 were set to be equal to zero in order to ensure symmetry about the origin. It should be noted that the rotational behaviour of U-FREI is not accounted for in this model.

Combining these two models together, the total force of the two models in parallel at any displacement can be found:

$$\begin{aligned} F_T(u) &= (k_1 + a_1)u + a_3 u^3 + a_5 u^5 && u < u_y \\ F_T(u) &= k_1 u_y + k_2(u - u_y) + a_1 u + a_3 u^3 + a_5 u^5 && u \geq u_y \end{aligned} \tag{3.3}$$

In total, this model contains six parameters that must be determined. These parameters do not have any inherent meaning with respect to the properties of the rubber or carbon fiber that were used to construct the isolator. To calculate these parameters, the effective stiffness and effective damping of a U-FREI must be

obtained, typically experimentally. Once determined, the error between the experimental and modeled effective stiffness and damping values are minimized. The unscragged value at each displacement amplitude is used to ensure that the model captures the largest stiffness value obtained from testing. This process must only be completed once for each isolator, since the six parameters are used to describe the entire hysteresis loop for any lateral displacement amplitude. The horizontal effective stiffness of each hysteresis loop is expressed as:

$$K_{horizontal,eff} = \frac{F_T(u_{max})}{u_{max}} \tag{3.4}$$

where u_{max} represents the maximum displacement of an individual hysteresis loop. The effective damping of each hysteresis loop is given as follows (Al-Anany et al. 2017):

$$\beta_{eff} = \frac{\left(k_1 u_y + k_2(u_{max} - u_y)\right) * 2\left(u - \frac{k_1 u_y + k_2(u_{max} - u_y)}{k_1}\right)}{2\pi k_{eff}(u_{max})^2} \qquad u_{max} \geq u_y \tag{3.5}$$

As mentioned, due to the Takeda model providing the only energy dissipation, the equation is only valid for displacements at or past the yield displacement.

3.3.2 Modeling U-FREI

The Takeda-Elastic model was used to determine the parameters required to describe the ¼-scale U-FREI specimen tested at room temperature. From this specimen, a proposed full-scale isolator was modeled. The U-FREI was geometrically scaled by a factor of four, while maintaining dynamic similitude requirements. The

resultant properties of the full-scale isolator compared to the ¼-scale experiment specimen are provided in Table 3.1.

Using the Takeda-Elastic Model obtained properties, the proposed full-scale isolator was input into OpenSees as a single degree-of-freedom and subjected to displacement-controlled cyclic loading. The effective stiffness and damping were calculated and compared to the scaled values obtained from the experimental results. As seen in Table 3.2, the stiffness values obtained from the model are within 2% at each displacement amplitude and the damping values are within 5% at each displacement amplitude. The hysteretic behaviour of the full-scale isolator is compared to the experimentally obtained hysteresis loops in Figure 3.4, where it can be seen that the full-scale isolator is in good agreement with the experimental data. The force in the figure has been normalized by the product of the shear modulus, G, and the isolator area, A, while the lateral displacements, u, have been normalized by the total height of rubber in the isolator, t_r. These results confirm the ability of the model to capture the behaviour of U-FREI.

3.3.3 Low Temperature Modeling of U-FREI

At low temperatures, it has been found that rubber not only increases in stiffness, but that it also has more energy dissipation resulting in hysteresis loops with greater area and larger effective damping ratios when subjected to cyclic testing (Kulak and Hughes 1993; Sciascetti et al. 2016; Sciascetti and Tait 2017). This is especially evident at large displacement amplitudes and makes modeling damping challenging. Despite the increase in energy dissipation, it was found that the Takeda-Elastic model

could still be used to adequately represent the behaviour of scaled U-FREI. As with the room temperature full-scale isolator, the low temperature full-scale isolators maintained stiffness values within 2% and damping values within 5% of values obtained experimentally. The parameters obtained through this process were used as starting values in order to create sets of equations that describe the behaviour of U-FREI over a range of temperatures and conditioning durations.

The two sets of equations that were created are for isolators conditioned for one day, from the temperatures of -18°C to -37°C and for isolators conditioned at -37°C from 1 to 28 days. This represents the effect of instantaneous thermal stiffening and stiffening due to crystallization, respectfully. The temperatures of -18°C and -26°C were not considered for the second set of equations as they displayed little to no change in properties between one and 14 days of conditioning. Both sets of equations were developed simultaneously using linear regression of the Takeda-Elastic parameters over the three tested temperatures of -18°C, -26°C and -37°C and the three conditioning durations of 1, 14 and 28 days. This created a separate equation for each of the six parameters that are used in the Takeda-Elastic model, where the only variable in each equation is temperature or duration. Since both equations can describe an isolator conditioned for 1 day at -37°C, the same parameter values are obtained for this case regardless of which set of equations was used. Similar to the room temperature model, the error of the effective stiffness and damping at each displacement amplitude between the experimental and the full-scale isolator was minimized.

The results of this process are two sets of intersecting equations that model full-scale U-FREI isolators. The equations are given as coefficients that are substituted into one of the following two linear equations:

$$P_{Temperature} = a_{T0} + a_{T1}T \qquad -18°C \geq T \geq -37°C \tag{3.6}$$

$$P_{Duration} = a_{D0} + a_{D1}D \qquad 1\ day \leq D \leq 28\ days \tag{3.7}$$

where the coefficients a, are provided in Table 3.3. The intercept coefficients are a_{T0} and a_{D0} and the slope coefficients are a_{T1} and a_{D1}. $P_{Temperature}$ is a placeholder for any of the six parameters used to describe isolators under the effects of instantaneous thermal stiffening. Temperature, T, is the only variable in Equation (3.6). $P_{Duration}$ is a placeholder for any of the six parameters used to describe isolators under the effects of low temperature crystallization. The conditioning duration, D, is the only variable in Equation (3.7). The *Duration* data set does not take into consideration the initial delay before the onset of crystallization as found to occur by Roeder et al. (1990). At shorter durations, between two to seven days, the effect of crystallization is over estimated. The labels '*Temperature'* and '*Duration'* will be used herein to represent the set of parameters, as well as the data set obtained from the above equations.

The *Temperature* set of equations provide effective stiffness and damping values that are within 5% of the experimental stiffness and damping values, while the *Duration* set of equations are within 8% of experimental values. The agreement of the hysteretic behaviour of the full-scale isolators using the given equations and the experimental data are provided in Figure 3.5. One of the findings from Toopchi-

Nezhad et al. (2008a) was that the rollover mechanism is stable when positive lateral tangential stiffness occurs throughout the hysteresis loop. This was enforced during the modeling of the full-scale isolators to ensure stability and can be seen in each plot of Figure 3.5.

3.4 BRIDGE MODEL

The numerical implementation of the U-FREI models into a three-span bridge was completed using the open source framework Open System for Earthquake Engineering Simulation (OpenSees). This software allows users to simulate the performance of structures that are subjected to ground motion. The model is based off of a three-span bridge proposed by Jangid (2004). The bridge deck rests upon rigid abutments at the ends and two, eight-metre tall, cylindrical piers spaced at 30 metres, having a diameter of 1.9 metres. The piers and deck were modeled to remain elastic throughout the duration of the simulation. This is accurate for the deck, as it is a capacity protected element and is required to remain in an elastic state (AASHTO 2011). With regards to the piers, isolation aims to reduce damage to structures by ensuring fuse elements, such as piers, remain elastic. As a result, non-linearity in the piers was not considered in this study.

Within OpenSees, the piers were modeled as fixed at the base. At the abutments, for the non-isolated case, the deck rested on frictionless bearings that restrain vertical movement. The pier weight was distributed using lumped masses. The bridge deck was split into 13 nodes and 12 segments, while each pier contained three nodes and two segments as illustrated in Figure 3.6. These elements were assigned 2% of critical

damping using initial stiffness proportional damping. This was done instead of Rayleigh damping in order to avoid amplification of damping in the first mode of the isolated structure (Ryan and Polanco 2008). The mass contained between each node was equally distributed between the confining nodes as point masses. The resulting fundamental period of the non-isolated bridge is 0.47 seconds, including the effects of the flexible deck. In the isolated bridge, U-FREI were placed at the top of each pier and abutment. It should be noted that the bearing design was not optimized for the bridge considered in this study. A total of 16 U-FREI were used in order to match the experimental testing conditions and maintain an approximate pressure of 7 MPa on each isolator. Based on the maximum and minimum stiffness values of the U-FREI, the isolated structure has an approximate fundamental period of 1.35 – 1.65 seconds at room temperature.

The bridge was subjected to a suite of 14 ground motions. They were selected and scaled to replicate the response spectrum of a bridge located in Montreal, Quebec. The National Building Code of Canada (NBCC) (2015) provided the seismic hazard values required to form the uniform hazard spectrum (UHS) for Montreal with a two percent probability of exceedance in 50 years and a site class of C. Montreal was chosen for this study as it is the largest city in Canada that is located in an area of high seismicity and experiences temperatures that are lower than -30°C (Statistics Canada 2016; Guay and Bouaanani 2016). The ground motions used were obtained through the PEER-NGA-West2 database and are presented in Table 3.4 (Pacific Earthquake Engineering Research Center 2017). The NGA-EAST database was not used, as scaling

factors were deemed to be too large. The fit of the ground motion spectra to that of the UHS is provided in Figure 3.7. To remain conservative, the mean response spectrum of the selected ground motions is either at or above the code response spectrum past the period of 0.4 seconds. The isolated bridge model was subjected to the suite of ground motions in both the transverse and longitudinal directions of the bridge deck. The resulting mean peak displacements, absolute accelerations and base shears in the two direction were within 2.5% of each other. The full-scale isolators are square and provide the same response in both directions, so only the transverse direction of the bridge is presented in this study.

Using the UHS provided by the NBCC, the displacements that were obtained from the model were compared to that of a simplified, iterative technique proposed by Tait et al. (2011) for evaluation purposes. The simplified iterative technique can be used to estimate displacements, accelerations and base shear of a single-degree-of-freedom (SDOF) model. Including U-FREI, the SDOF displacements were estimated to be 64.4 mm, which is less than a two percent difference over the bridge model mean value of 63.5 mm. The absolute acceleration provided by the SDOF were 0.100g, while the bridge model provided a mean peak acceleration of 0.103g. The peak base shear estimate from the SDOF model was only 7.5% greater than that of the bridge model.

3.5 RESULTS

The following data has been collected and presented to highlight the effect of low temperature on U-FREI. Both bridges, isolated and non-isolated, were subjected to the 14 scaled ground motions provided above in the transverse direction. For the

isolated bridge, the suite of ground motions was run a total of 11 times. The first being at room temperature (RT) using the parameters provided in Table 3.1 and the remainder were at low temperatures using parameters provided by Equations 3.6 and 3.7. This provided two sets of data, the *Temperature* U-FREI and the *Duration* U-FREI, as defined in Section 3.3.3. The *Temperature* set provides data on the effect of instantaneous thermal stiffening, while the *Duration* set provides data on the effect of low temperature crystallization on the response of a three-span bridge outfitted with U-FREI. Using time history analysis, the response quantities that are being evaluated are the peak absolute acceleration of the bridge deck, the peak deck displacement, as well as the peak base shear at the bottom of the bridge pier.

The peak response quantities have been summarized in the following two sections for the suite of ground motions that were considered. The peak response quantity of the isolated bridge for each earthquake was normalized by the corresponding non-isolated peak response quantity. The mean response of the normalized values over the suite of ground motions was then calculated.

The figures found in the following two sub-sections have two distinct features. On the right side of the figure, the response quantity of the non-isolated bridge is provided for reference. The dark black line is the mean value found from averaging the normalized responses at each temperature.

3.5.1 Data Set | *Temperature*

The effect of instantaneous thermal stiffening has been shown to cause U-FREI to exhibit increased stiffness and damping properties (Sciascetti and Tait 2017). These changes were captured in the updated Takeda-Elastic model over the temperatures of 20°C to -37°C for a single day of conditioning.

As expected, Figure 3.8 shows that the peak deck displacement of the isolated bridge at room temperature is much greater than that of the non-isolated bridge. On average, there was a 2.6 times increase in displacement. Correspondingly, the demand on the piers decreased significantly, with the mean peak displacement at the top of the pier reduced to 10% of the non-isolated value. At the lowest temperature of -37°C, the peak displacement is greatly reduced. For select ground motions, the peak deck displacement is actually less than the corresponding non-isolated deck displacements. However, on average, the peak displacement increased by 11%. The mean pier-top peak displacements of the isolated bridge only increased by less than 1% of the non-isolated value over the range of temperatures tested.

The absolute accelerations of the isolated bridge deck in Figure 3.9 are similar across all temperatures, where a large decrease in absolute accelerations can be seen compared to the non-isolated bridge. The average reduction in acceleration is approximately 77-80% across all temperatures.

The last response quantity, peak base shear, presents similar results. In Figure 3.10 the non-isolated peak base shear values have been normalized by the weight of

the bridge, W_B. For the non-isolated bridge, half of the total base shear is resisted by each of the two bridge piers. In the isolated bridge, isolators are placed at the abutments as well as at the piers. Forces in the bridge are distributed among the two piers and two abutments, unlike in the non-isolated bridge. This in itself reduces the base shear values in a single pier. This is one of the benefits of an isolated bridge, since the ends of the bridge have a reliable way to transmit forces to the abutments. Referring to the figure, it can be seen that the peak base shear remains fairly constant with a decrease in temperature. The peak base shear at all temperatures, on average, is 11.5% of the non-isolated peak base shear. This base shear response corresponds with the results provided in Figure 3.8. The peak pier-top displacements were minimal, causing small peak base shear values.

When U-FREI are subjected to low temperatures, it has been found that there is an associated increase in stiffness that is paired with an increase in energy dissipation (Sciascetti and Tait 2017). The decrease in displacement can be directly attributed to this increase in stiffness experienced by the isolators at low temperatures. The same force that is caused by each ground motion can be accommodated with less displacement as a result. For example, at -37°C, U-FREI exhibit a damping ratio more than twice that of room temperature (Sciascetti and Tait 2017). A large damping ratio helps to limit the absolute accelerations due to low temperature stiffness increases. Thus, the forces transferred into the bridge piers are also greatly reduced.

These results indicate that instantaneous thermal stiffening down to a temperature of -37°C does not significantly affect the performance of a bridge structure

isolated with U-FREI. Further decreases in temperature will result in a further reduction of displacement and increases in absolute acceleration and base shear. As the glass transition temperature is approached and passed, the stiffness of the elastomeric isolators will increase significantly (Roeder et al. 1989; Bukhina and Kurlyand 2007). However, further experimental testing would be required to determine the glass transition temperature and any change in behaviour of U-FREI.

3.5.2 Data Set | *Duration*

This data set presents the effect of low temperature crystallization on the performance of the isolated three-span bridge. It has been shown that even more drastic changes in stiffness and damping occur as the length of low temperature conditioning is increased (Sciascetti and Tait 2017). The following figures will depict the trends associated with conditioning at -37°C for zero to 28 days. Zero days of conditioning represents the room temperature specimen.

Figure 3.11 shows that the peak deck displacement decreases as the length of time conditioned at -37°C increases. It can be observed that the largest decrease in displacement occurs between zero and one day of conditioning. This large jump is due to instantaneous thermal stiffening as the bearing drops from room temperature to -37°C and was depicted in Figure 3.8. At approximately 4 days, the average isolated peak deck displacement is equal to that of the non-isolated bridge. As the conditioning duration approaches 28 days, the slope of the mean response curve reduces, as if it will start to plateau upon further conditioning. The slope of the mean displacement curve between 1 and 4 days is four times greater than the slope of the curve between 25 and

28 days of conditioning. At 28 days, the deck displacement is 48% of the non-isolated bridge and the pier-top displacement increased from 10% to 22% of the non-isolated bridge values.

Although Figure 3.11 shows instantaneous thermal stiffening as contributing more to the decrease in peak deck displacement, Figure 3.12 indicates that crystallization causes the larger increase in peak absolute acceleration. The normalized peak values jump from 22% to 53% of the non-isolated bridge values, between 1 and 28 days of conditioning. On average, there was still a 47% decrease in the acceleration felt by the bridge deck.

Similar to the absolute acceleration response, in Figure 3.13, the peak base shear is shown to be affected by crystallization more than instantaneous thermal stiffening. After one day of conditioning at -37°C, the peak base shear is 11% of the non-isolated value, but over 28 days of conditioning, the peak base shear more than doubles to 24% of the mean non-isolated peak base shear value.

When subjected to low temperatures for an extended period of time, U-FREI exhibit an increase in stiffness, in addition to what occurs rapidly upon first being subjected to low temperatures (Sciascetti and Tait 2017). This stiffness increase can be seen to cause the peak deck displacement to decrease and the peak absolute acceleration to increase. The reduction in slope of the mean displacement response curve as 28 days is approached may indicate that the stiffness of the isolator is reaching its maximum conditioned value. This is in agreement with previous research on rubber that indicates

elastomers reach an equilibrium point during the crystallization process, where no further crystals form and stiffness no longer increases (Stevenson and Maxwell 1986). Roeder et al. (1989) recommended that bearings need not be conditioned past 28 days as they found a plateau in stiffness occurred during their research as well.

From these results, it has been shown that the effect of crystallization on the performance of the isolated bridge is large. The performance, in even the most extreme case, is better than that of a non-isolated bridge. The result obtained by Sciascetti and Tait (2017), where the isolator conditioned for 28 days at -37°C did not pass the criteria outline by AASHTO, has been shown to be capable of providing acceptable performance. This decision was concluded from the reduction in both absolute acceleration and base shear that was provided by the isolated bridge after the 28 days of conditioning. The demand on the piers was reduced by more than half, indicating that damage in the piers could be significantly reduced or completely eliminated. Each case must be considered separately however. For example, a 50% reduction in absolute accelerations, as provided by U-FREI after 28 days of conditioning, may not be acceptable, even though pier deflection and base shear criteria are met.

3.6 RESPONSE TO A SUDDEN DECREASE IN TEMPERATURE

In regards to the location that this bridge model was situated, Montreal can achieve temperatures that are close to -37°C, but cannot sustain them for a long period of time (Guay and Bouaanani 2016). It would not be warranted to need isolators to perform adequately past 2 days at -37°C, and 8 days at -15°C. Crystallization at the latter temperature would provide very little change in response quantities and

performance as found experimentally by Sciascetti and Tait (2017). With this knowledge, the *Temperature* dataset presented in Section 3.5.1 could be used to provide simulated responses if isolating a bridge structure in Montreal. The following sub-sections provide simulated ground motion responses in the event that Montreal is subjected to a sudden decrease in temperature to -37°C.

3.6.1 Typical Response Histories

The following four figures give the representation of typical response histories for a single representative ground motion. For comparison, the room temperature bridge is displayed to the left of the bridge isolated with U-FREI conditioned at -37°C for a single day. Figure 3.14 depicts the large change in the peak deck displacement response between the isolated and non-isolated bridge, as well as between room and low temperature conditioning. Due to the restoring forces of the isolators, there are zero residual displacements present in the isolated bridges. The long, distinct cycles of the room temperature bridge depict what would be expected of an isolated structure. For the low temperature isolated bridge, there appears to be a higher frequency present in the response history, along with an observable decrease in the amplitude. This is indicative of the increase in stiffness experienced by the U-FREI at -37°C. In Figure 3.15 and Figure 3.16, a large decrease in absolute acceleration and base shear can be seen compared to the non-isolated bridge. In terms of response amplitude, the low temperature bridge performs similarly to that of the room temperature isolated bridge. The difference between the two is the higher frequency content in both low temperature responses. As the stiffness of the U-FREI increases, the high frequencies present in the

ground motion become more prevalent in the response histories. Figure 3.17 provides the change in the hysteretic behaviour of the isolators placed between the bridge deck and pier. As observed in the displacement time histories, the isolator conditioned at -37°C for a single day is only displaced to 0.4 t_r compared to 0.95 t_r at room temperature.

3.6.2 Peak Response Summary

The following figures provide aggregated results of the peak response parameters for multiple hazard levels according to those outlined in the Canadian Highway Bridge Design Code (2014). The code outlines three hazard levels in terms of the probability that a ground motion will exceed the specified spectral accelerations in 50 years (PE_{50}). A larger value represents a lower hazard level. They are 10% PE_{50}, 5% PE_{50} and 2% PE_{50}, with the 2% PE_{50} matching the Uniform Hazard Spectra of the NBCC. The 5% and 10% PE_{50} spectral acceleration values were obtained as interpolated values from the National Building Code of Canada, 2015 (Natural Resources Canada 2017). Each of the 14 ground motions provided in Section 3.4 were scaled to the hazard levels of 5% and 10% PE_{50}. The 2% PE_{50} data is the same as that obtained from the Uniform Hazard Spectra (UHS), but the mean values presented in this section have not been normalized by the corresponding non-isolated response.

The mean peak absolute acceleration response of the bridge deck from the suite of ground motions for each hazard level is provided in Figure 3.18. At 2% PE_{50}, the isolated accelerations are approximately 17% of the non-isolated bridge, with the room temperature (RT) isolated response slightly less than the conditioned bridge at -37°C. At 5% PE_{50}, the non-isolated and room temperature responses are approximately half

of their 2% PE_{50} response. The -37°C isolated response only decreases by 25%. At 10% PE_{50}, the non-isolated and room temperature responses decrease by 40%, while the -37°C average response only decreases by 14%. This indicates that with a decrease in hazard level, the ratio between the isolated and non-isolated bridge remains at approximately 0.18 for the full-scale isolator used in this model. As the hazard level decreases for the low temperature isolated bridge, the ratio of the low temperature isolated and non-isolated bridge increases. The ratio increases from 0.19 at 2% PE_{50} to 0.38 at 10% PE_{50}. However, although the degree of isolation varies with decreasing hazard levels at low temperatures, the absolute acceleration values are still lower than both isolated bridges at the 2% PE_{50} hazard level.

Figure 3.19 provides the same comparison as Figure 3.18, but for the mean peak base shear response. The base shear has been normalized by the weight of the bridge, W_b, as in the previous sections. The same trend that occurred with the absolute accelerations is visible with the mean peak base shear values. The ratio between the room temperature isolated and non-isolated base shear values at each hazard level is consistent at 0.10. While the ratio for the low temperature response increases with a decrease in hazard level. At 2% PE_{50}, the ratio is 0.10 and rises to 0.18 at 10% PE_{50}.

In terms of displacement, Figure 3.20 and Figure 3.21 provide the peak displacement response of the U-FREI at each hazard level for each of the 14 ground motions. The peak displacements have been normalized by the total height of rubber in a full-scale isolator, t_r. The first figure shows a large increase in displacement compared to the deck displacement of the non-isolated bridge. As the hazard level

decreases, the ratio of isolated divided by non-isolated response decreases. At 2% PE_{50} the ratio is 2.33, but at 10% PE_{50}, it drops to 1.65. At room temperature, the isolators do not provide the same degree of isolation across all hazard levels. However, even at 10% PE_{50}, the non-isolated response is only greater in three instances by a small margin. In these cases, the displacement of the piers is still less than 0.04 t_r and as shown in Figure 3.19, the base shear in each pier is quite low, indicating limited or no damage to the piers. In comparison, Figure 3.21 shows the large decrease in isolator displacement with the bridge conditioned at -37°C. At 2% PE_{50} the average displacements are approximately the same, with many of the isolated responses less than the non-isolated responses. At 10% PE_{50}, the ratio for the isolated bridge drops to 0.54 times the average non-isolated response values. From the figure, it can be seen that at this hazard level, every isolated displacement response is less than the non-isolated value.

3.7 SUMMARY AND CONCLUSIONS

The goal of this study was to determine the effectiveness and adequacy in performance provided by a bridge isolated with unbonded, fiber-reinforced elastomeric isolators (U-FREI) located in a cold, Northern climate. In order to accomplish this, an updated non-iterative model for U-FREI, that accounts for the effect of temperature and conditioning duration, was developed. U-FREI at temperatures between -18°C and -37°C, along with U-FREI conditioned for up to 28 days were included in the model. It was found that the updated U-FREI model accurately provides a way to account for the effects of temperature on the hysteretic behaviour. Effective stiffness and damping

values are within 8% of experimental results at all temperatures and conditioning durations considered.

This U-FREI model was then used to isolate a three-span bridge subjected to a suite of 14 ground motions in the transverse direction. Time history analysis was conducted and the three, main response parameters examined were peak deck displacement, peak absolute acceleration, and peak pier base shear. It was determined that the isolation of the three-span bridge presented in this study at room temperature reduces the seismic demand on bridge piers by allowing displacements to be accommodated by the isolation system. This in turn limits the maximum absolute acceleration felt by the bridge.

Instantaneous thermal stiffening (*Temperature* data set) was shown to have the largest effect on the peak deck displacement. When compared to the room temperature isolated bridge, the deck displacements decreased by 56% due to thermal stiffening, but only decreased an additional 25% due to crystallization (*Duration* data set). This indicates that displacements are affected more by stiffness induced by low temperatures and not conditioning durations.

The opposite was found to be true for the peak absolute accelerations. Instantaneous thermal stiffening only caused an 8% increase from the room temperature value, but crystallization caused a 2.5 times increase at 28 days. Despite the large effect that long conditioning durations have on absolute accelerations, when compared to the accelerations of the non-isolated bridge, they were still 47% less.

The peak base shear values were found to remain near constant due to thermal stiffening compared to the room temperature isolated bridge. As the conditioning duration was increased and crystallization occurred, the peak base shear values increased 2.1 times the room temperature value. However, this increase only represented 25% of the base shear experienced by the piers in the non-isolated bridge. This performance shows that there is still a benefit to isolating with U-FREI at extreme temperature conditions.

The bridge model was then used to evaluate the response parameters at additional hazard levels of 5% and 10% probability of exceedance in 50 years. In terms of absolute accelerations and base shear, the degree of isolation between the room temperature isolated and non-isolated bridge remained constant. It was found that a sudden decrease in temperature to -37°C caused a decrease in the degree of isolation at lower performance levels. This is also the case with both the room temperature and low temperature isolated bridges with respect to peak isolator displacement. As the hazard level was increased, the ratio of the isolated to the non-isolated bridge also decreased. It was observed that the lower hazard levels resulted in lower response parameters in general and that a decrease in the response of the isolation system compared to the non-isolated bridge did not correspond with a decrease in effectiveness. It is expected that the forces and displacements in the piers would result in little to no damage to the bridge piers.

The results that have been presented are representative of the bridge configuration described and the suite of ground motions selected. In order to apply

these results more generally, further bridge configurations should be evaluated. These results are indicative of the performance that U-FREI can provide, even in cold, northern climates. They have been shown to adequately isolate a three-span bridge at multiple temperatures and conditioning durations, while effectively limiting forces being transferred to the bridge piers.

3.8 REFERENCES

AASHTO. 2011. "Guide Specifications for LRFD Seismic Bridge Design." Washington, D.C.: American Association of State Highway and Transportation Officials.

AASHTO. 2016. "M 251-06 Standard Specification for Plain and Laminated Elastomeric Bridge Bearings." Washington, D.C.: American Association of State Highway and Transportation Officials.

Al-Anany, Y.M., Engelen, N.C. Van, and Tait, M.J. 2015. "Vertical and Lateral Behavior of Unbonded Fiber-Reinforced Elastomeric Isolators." *Journal of Composite Structures*, no. 1: 1–11.

Al-Anany, Y.M., Moustafa, M.A., and Tait, M.J. 2017. "Modeling and Evaluation of a Seismically Isolated Bridge Using Unbonded Fiber Reinforced Elastomeric Isolators." *Earthquake Spectra* In-Press.

Al-Anany, Y.M., and Tait, M.J. 2016. "An Experimental Study of the Vertical and Rotational Behaviour of Unbonded Fiber- Reinforced Elastomeric Isolators (U-FREI) for Bridge Applications,." *Composites Part B: Engineering*.

Al-anany, Y.M., and Tait, M.J. 2017a. "Experimental Assessment of Utilizing Fiber Reinforced Elastomeric Isolators as Bearings for Bridge Applications." *Composites Part B: Engineering* 114 (1): 373–85.

Al-Anany, Y.M., and Tait, M.J. 2017b. "Fiber Reinforced Elastomeric Isolators for the Seismic Isolation of Bridges." *Composite Structures* 160. Elsevier Ltd: 300–311.

Al-Anany, Y.M., Tait, M.J., Torrie, M., and Sciascetti, A.N. 2016. "The Vertical, Rotational and Lateral Response of Unbonded Fiber Reinforced Elastomeric Isolators." In *Resilient Infrastructure*, 1–10. London.

Buckle, I.G., Al-Ani, M., and Monzon, E. 2011. "Seismic Isolation Design Examples of Highway Bridges." *NCHRP Progect: 20-7*.

Buckle, I.G., Constantinou, M.C., Dicleli, M., and Ghasemi, H. 2006. *Seismic Isolation of Highway Bridges*. *MCEER-06-SP07*. Buffalo, NY: Multidisciplinary Center for Earthquake Engineering Research.

Bukhina, M.F., and Kurlyand, S.K. 2007. *New Concepts in Polymer Science: Low-Temperature Behaviour of Elastomers*. Boca Raton: CRC Press.

Canadian Commission on Buildings and Fire Codes. 2015. *National Building Code of Canada*. Vol. 2. National Research Council of Canada.

CAN/CSA-S6. 2014. "Canadian Highway Bridge Design Code (CHBDC)." Ontario: Canadian Standard Association.

Ghobarah, A., and Ali, H.M. 1988. "Seismic Performance of Highway Bridges." *Engineering Structures* 10: 157–66.

Guay, L., and Bouaanani, N. 2016. "Assessment of Low Temperature Exposure for Design and Evaluation of Elastomeric Bridge Bearings and Seismic Isolators in Canada." *Canadian Joural of Civil Engineering* 43: 851–63.

Jangid, R.S. 2004. "Seismic Response of Isolated Bridges." *Journal of Bridge Engineering* 9 (2): 156–66.

Jangid, R.S. 2008. "Stochastic Response of Bridges Seismically Isolated by Friction Pendulum System." *Journal of Bridge Engineering* 13 (4): 319–30.

Kulak, R.F., and Hughes, T.H. 1993. "Frequency and Temperature Dependence of High Damping Elastomers." Oak Ridge, TN, USA: Office of Scientific and Technical Information.

Love, J.S., Tait, M.J., and Toopchi-Nezhad, H. 2011. "A Hybrid Structural Control System Using a Tuned Liquid Damper to Reduce Wind Induced Motion of a Base Isolated Structure." *Engineering Structures* 33 (3): 738–46.

Natural Resources Canada. 2017. "2015 NBCC Seismic Hazard Calculator." Accessed July 7. http://www.earthquakescanada.nrcan.gc.ca/index-en.php.

Osgooei, P.M., Tait, M.J., and Konstantinidis, D. 2017. Non-iterative computational model for fiber-reinforced elastomeric isolators. *Engineering Structures*, issued 2017.

Pacific Earthquake Engineering Research Center. 2017. "PEER Ground Motion DataBase." University of California, Berkeley. Accessed June 6. http://ngawest2.berkeley.edu/site.

Raaf, M.G.P. de, Tait, M.J., and Toopchi-Nezhad, H. 2011. "Stability of Fiber-Reinforced Elastomeric Bearings in an Unbonded Application." *Journal of Composite Materials* 45 (February): 1873–84.

Roeder, C.W., Stanton, J., and Feller, T. 1989. "Low Temperature Behaviour and Acceptance Criteria for Elastomeric Bridge Bearings." Washington, D.C., USA: Transportation Research Board.

Roeder, C.W., Stanton, J., and Feller, T. 1990. "Low-Temperature Performance of Elastomeric Bearings." *Journal of Cold Regions Engineering* 4 (3): 113–32.

Ryan, K.L., and Polanco, J. 2008. "Problems with Rayleigh Damping in Base-Isolated Buildings." *Journal of Structural Engineering*, no. November: 1780–84.

Sciascetti, A.N., Al-Anany, Y.M., and Tait, M.J. 2016. "The Effect of Temperature on the Lateral Response of Unbonded Fiber-Reinforced Elastomeric Isolators." In *Resilient Infrastructure*, 1–10. London.

Sciascetti, A.N., and Tait, M.J. 2017. "The Effect of Temperature on the Lateral, Vertical and Rotational Response of Unbonded Fiber-Reinforced Elastomeric Isolators."

Statistics Canada. 2016. "Population and Dwelling Count Highlight Tables, 2016 Census." http://www12.statcan.gc.ca/census-recensement/2016/dp-pd/hlt-fst/pd-pl/Table.cfm?Lang=Eng&T=307&S=3&O=D.

Stevenson, A., and Maxwell, D.L. 1986. "Low Temperature Stiffening of Structural Rubber Bearings." In *International Rubber Conference*, 424–30. Goteborg, Sweden: The Swedish Institution of Rubber Technology.

Tait, M.J., Drysdale, R.G., Toopchi-Nezhad, H., Foster, B., and Raaf, M.G.P. de. 2011. "Seismic Isolation of Residential Wood Frame and Low-Rise Masonry Buildings." Hamilton, Canada.

Takeda, T., Sozen, M., and Nielsen, N. 1970. "Reinforced Concrete Reponse to Simulated Earthquakes." *Journal of Structural Division* 96 (12): 2557–73.

Toopchi-Nezhad, H., Drysdale, R.G., and Tait, M.J. 2009. "Parametric Study on the Response of Stable Unbonded-Fiber Reinforced Elastomeric Isolators (SU-FREIs)." *Journal of Composite Materials* 43 (15): 1569–87.

Toopchi-nezhad, H., Tait, M.J., and Drysdale, R.G. 2009. "Simplified Analysis of a Low-Rise Building Seismically Isolated with Stable Unbonded Fiber Reinforced Elastomeric Isolators Simplified Analysis of a Low-Rise Building Seismically Isolated with Stable Unbonded Fiber Reinforced Elastomeric Isolators." *Canadian Joural of Civil Engineering*.

Toopchi-Nezhad, H., Tait, M.J., and Drysdale, R.G. 2008. "Testing and Modeling of Square Carbon Fiber-Reinforced Elastomeric Seismic Isolators." *Structural Control and Health Monitoring* 15: 876–900.

Van Engelen, N.C., Osgooei, P.M., Tait, M.J., and Konstantinidis, D. 2014. "Experimental and Finite Element Study on the Compression Properties of Modified Rectangular Fiber-Reinforced Elastomeric Isolators." *Engineering Structures* 74. Elsevier Ltd: 52–64.

Wang, Y.P., Chung, L.L., and Liao, W.H. 1998. "Seismic Response Analysis of Bridges Isolated with Friction Pendulum Bearings." *Earthquake Engineering and Structural Dynamics* 27 (10): 1069–93.

Table 3.1: Specimen and model parameters

	Parameter		¼ Scale Specimen	Full-Scale Isolator
Geometric Properties	Length (mm)		64	256
	Isolator height (mm)		19	76
	Rubber height, t_r (mm)		18	72
	Aspect Ratio		3.37	3.37
	Shape Factor		5.52	5.52
Takeda-Elastic Model Properties	k_1	(N/mm)	524.09	2096.36
	k_2	(N/mm)	35.81	143.24
	u_y	(mm)	0.61	2.44
	a_1	(N/mm)	148.52	594.08
	a_3	(N/mm^3)	-0.095	-0.024
	a_5	(N/mm^5)	7.47×10^{-5}	1.17×10^{-6}

Table 3.2: Room temperature comparison of experimental specimen to full-scale isolator

Displacement Amplitude (u/t_r)	Stiffness (N/mm)			Damping (%)		
	Experimental	Full-Scale	Error (%)	Experimental	Full-Scale	Error (%)
0.25	1020	1000	-2.0	10.7	10.6	-1.4
0.50	852	840	-1.4	9.4	9.0	-4.2
0.75	747	762	2.0	8.8	8.5	-2.7
1.00	694	708	2.0	8.0	8.4	5.0
1.50	679	665	-2.0	8.3	8.1	-2.0

Table 3.3: Intercept and slope coefficients for low-temperature equations.

		Temperature		Duration	
P		a_{T0}	a_{T1}	a_{D0}	a_{D1}
k_1	(N/mm)	-15719.2	-1359.6	33345.2	924.8
k_2	(N/mm)	210.5	-5.2×10^{-1}	240.1	-10.9
u_y	(mm)	8.3×10^{-1}	3.7×10^{-3}	6.5×10^{-1}	2.8×10^{-2}
a_1	(N/mm)	814.3	6.1	557.8	27.5
a_3	(N/mm^3)	-4.8×10^{-2}	-1.0×10^{-3}	-6.1×10^{-3}	-5.5×10^{-3}
a_5	(N/mm^5)	1.4×10^{-6}	-1.2×10^{-9}	1.2×10^{-6}	2.6×10^{-7}

Table 3.4: Selected ground motions from PEER-NGA-West2 database.

Record ID	Record Name	Year	Station Name	Magnitude	Scale Factor
88	San Fernando	1971	Santa Felita Dam (Outlet)	6.61	2.71
187	Imperial Valley	1979	Parachute Test Site	6.53	1.40
291	Irpinia	1980	Rionero In Vulture	6.90	1.80
734	Loma Prieta	1989	APEEL 3E Hayward CSUH	6.93	2.00
762	Loma Prieta	1989	Fremont - Mission San Jose	6.93	1.42
921	Big Bear	1992	Palm Springs Airport	6.46	2.77
976	Northridge	1994	Hacienda Heights - Colima	6.69	2.72
1144	Gulf of Aqaba	1995	Eilat	7.20	1.81
1776	Hector Mine	1999	Desert Hot Springs	7.13	1.88
3471	Chi-Chi	1999	TCU075	6.30	2.03
3927	Tottori	2000	OKYH09	6.61	2.20
3994	San Simeon	2003	San Luis Obispo	6.52	1.85
4869	Chuetsu-oki	2007	Kawaguchi	6.80	1.06
5779	Iwate	2008	Sanbongi Osaki City	6.90	1.06

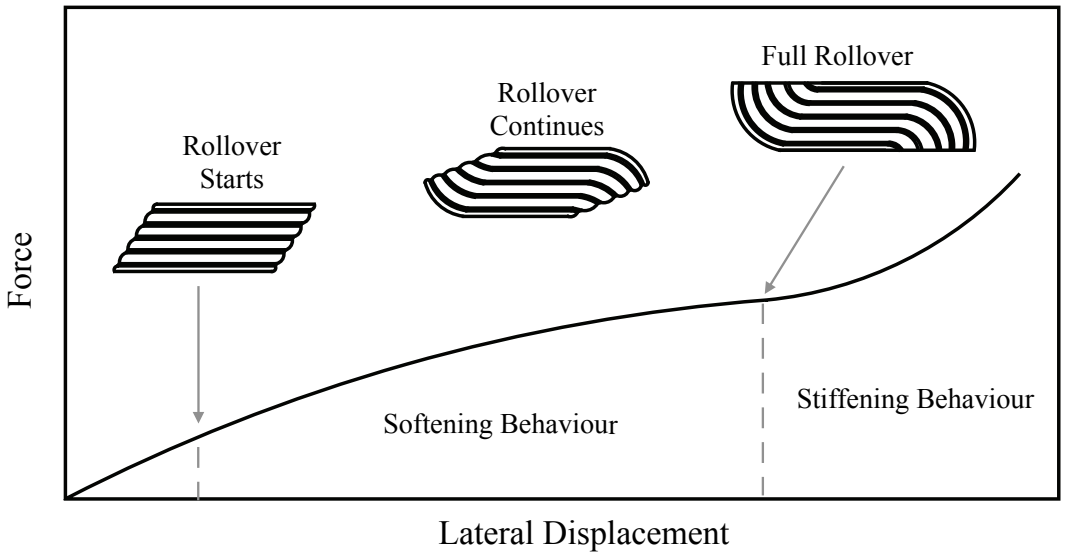

Figure 3.1: Phases of U-FREI load displacement curve.

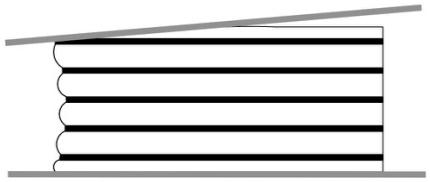

Figure 3.2: Lift-off in an unbonded-FREI.

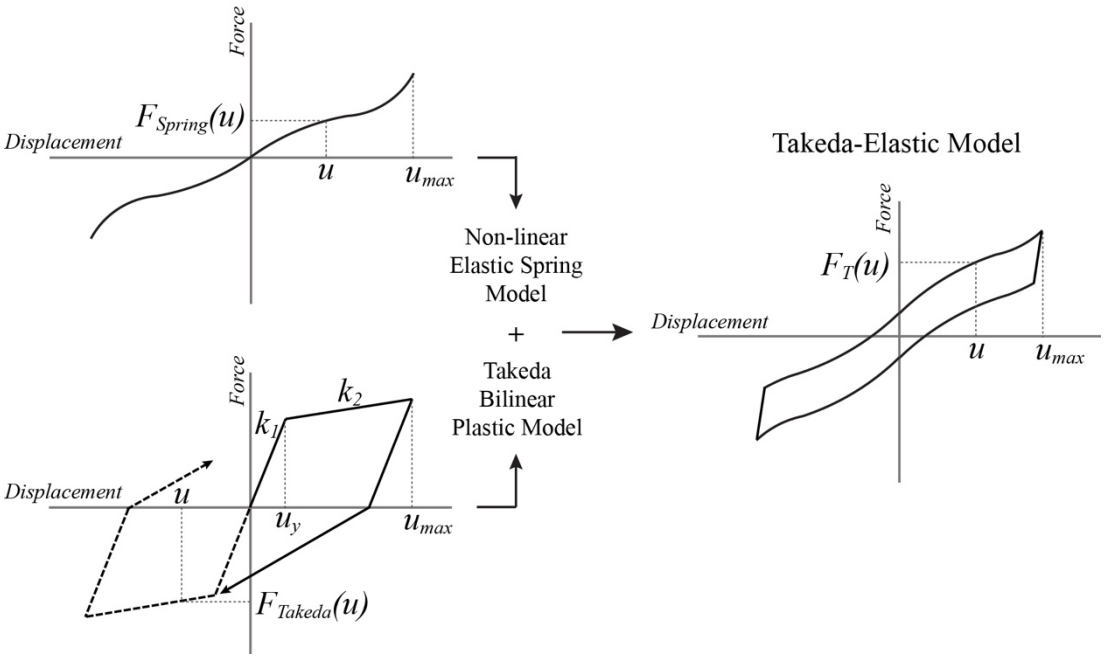

Figure 3.3: Takeda-Elastic Model depicted as the combination, in parallel, of the Non-linear Elastic Spring Model and the Takeda Bilinear Plastic Model.

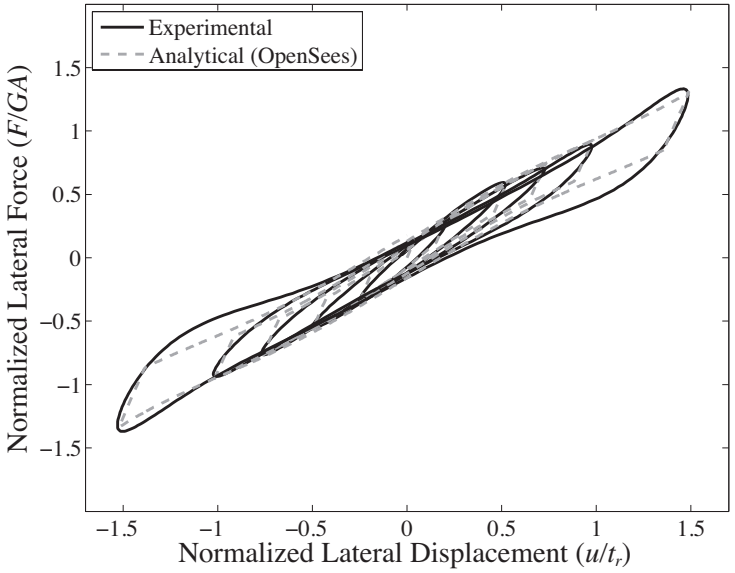

Figure 3.4: Room temperature normalized hysteresis loop comparison.

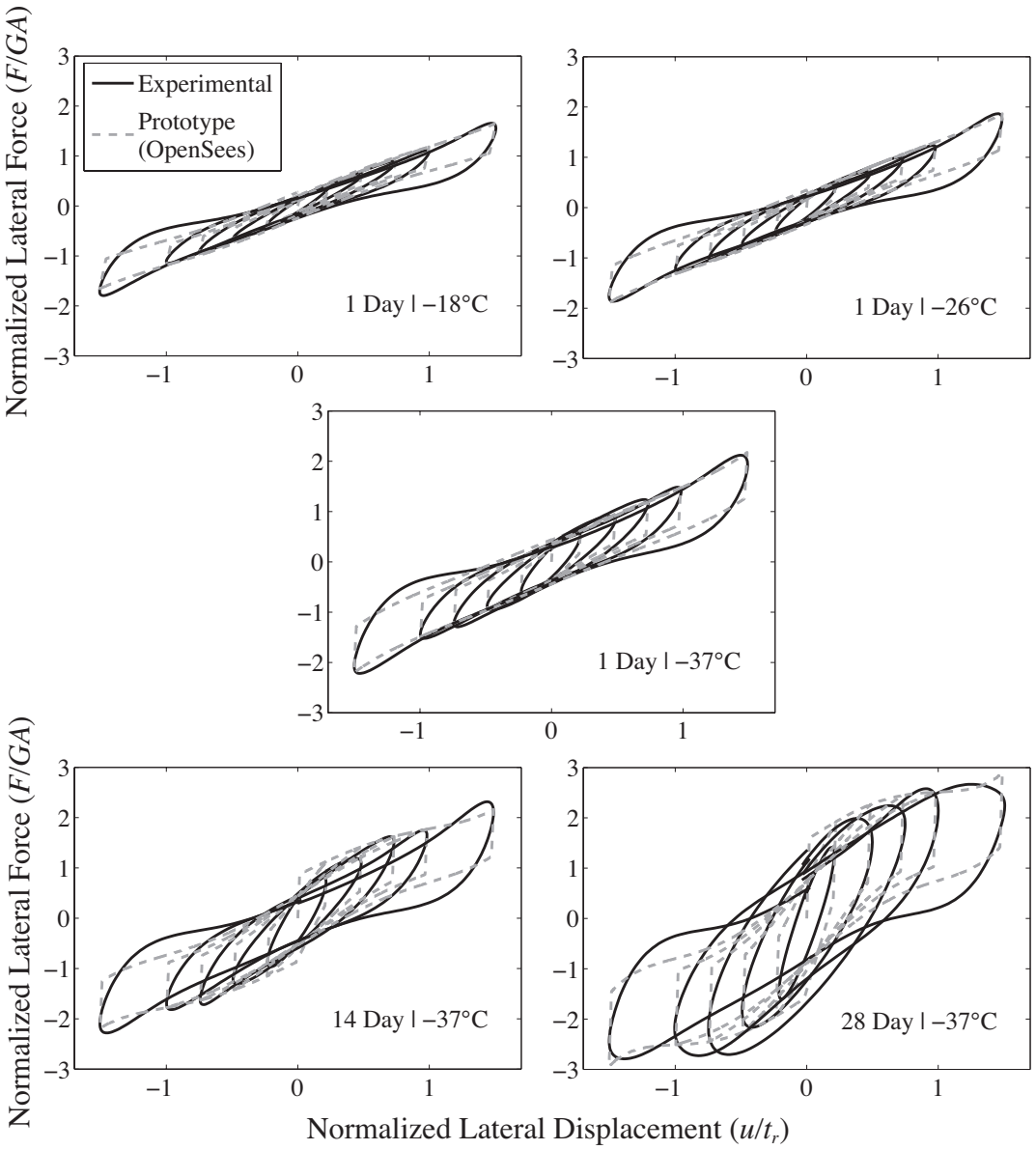

Figure 3.5: Normalized lateral hysteretic behaviour comparison.

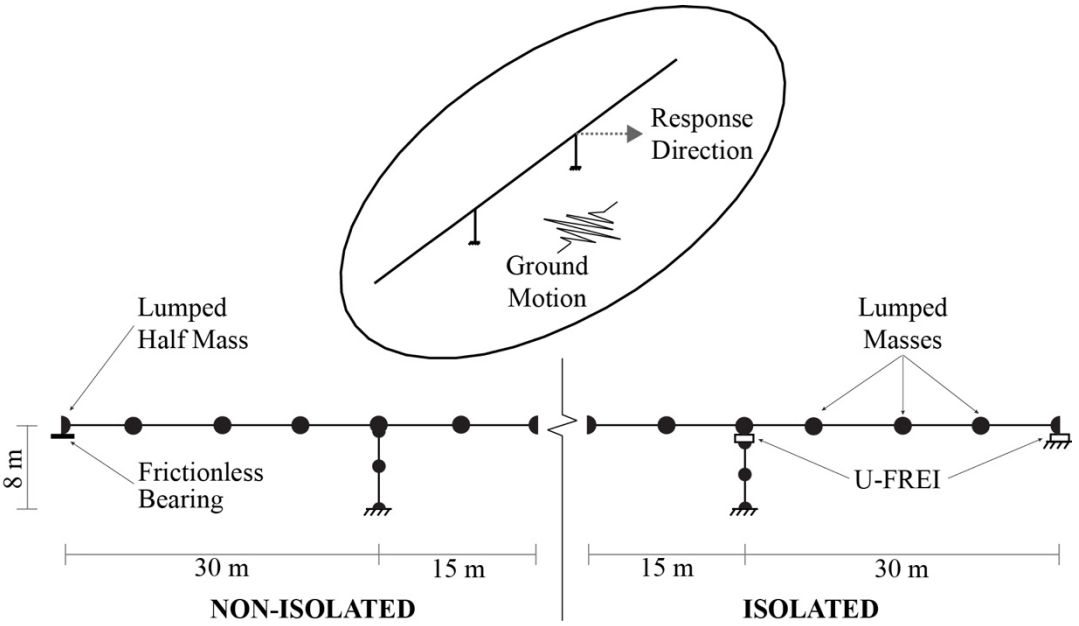

Figure 3.6: Non-isolated vs isolated bridge model (half of each depicted).

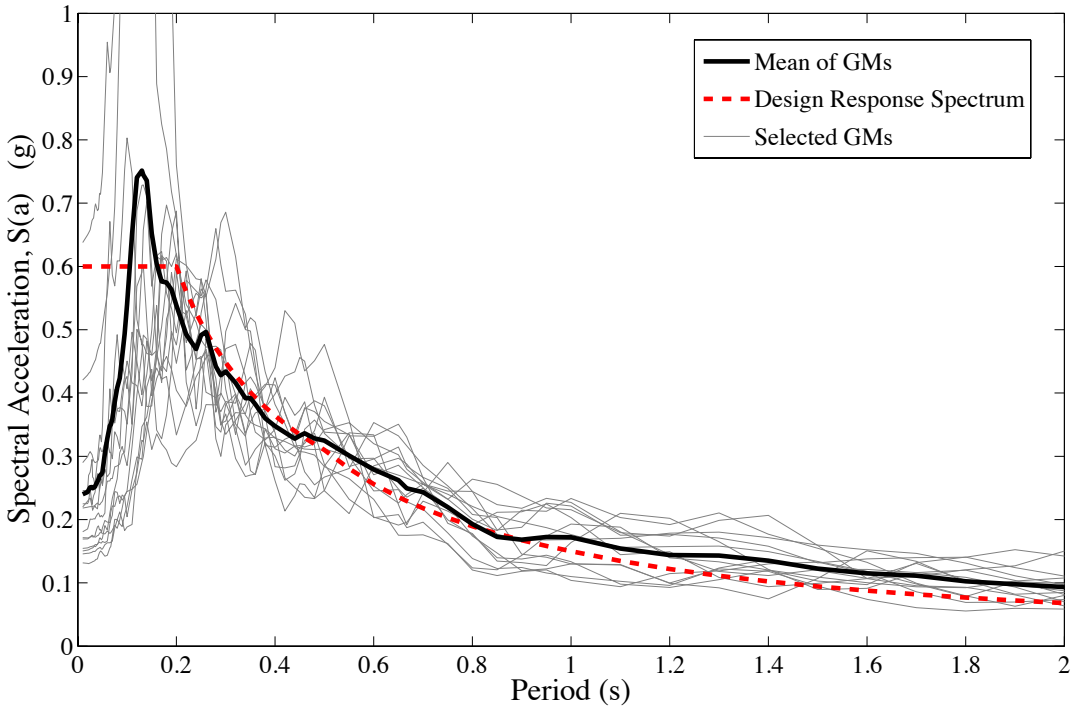

Figure 3.7: Uniform hazard spectrum for Montreal, Quebec (5% damping) compared to the selected scaled ground motions and their mean.

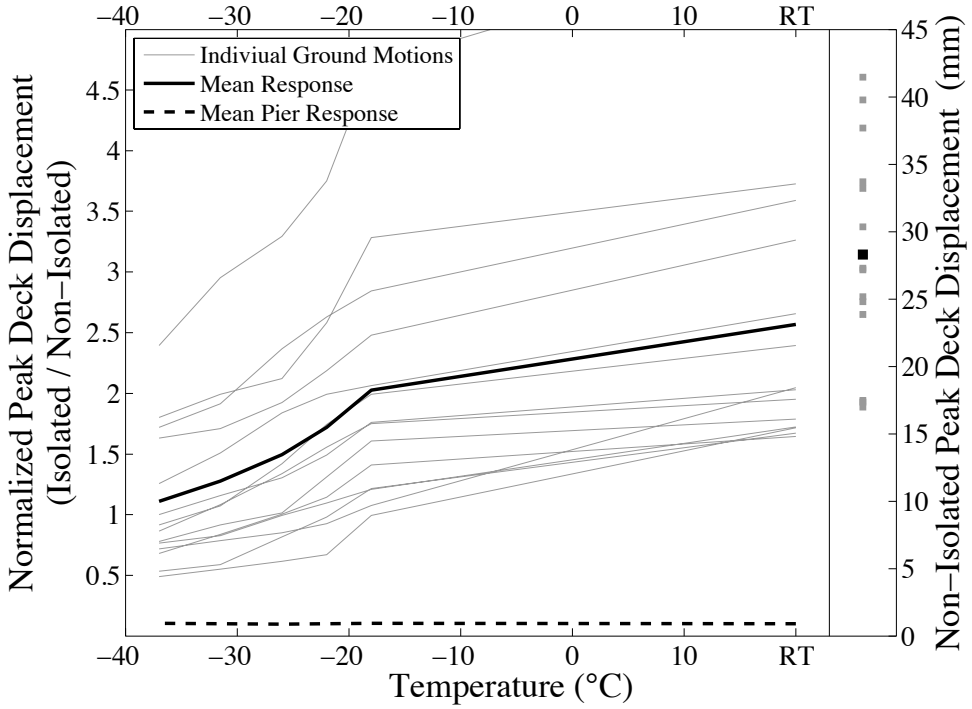

Figure 3.8: The change in peak deck displacement associated with low temperature conditioning for one day.

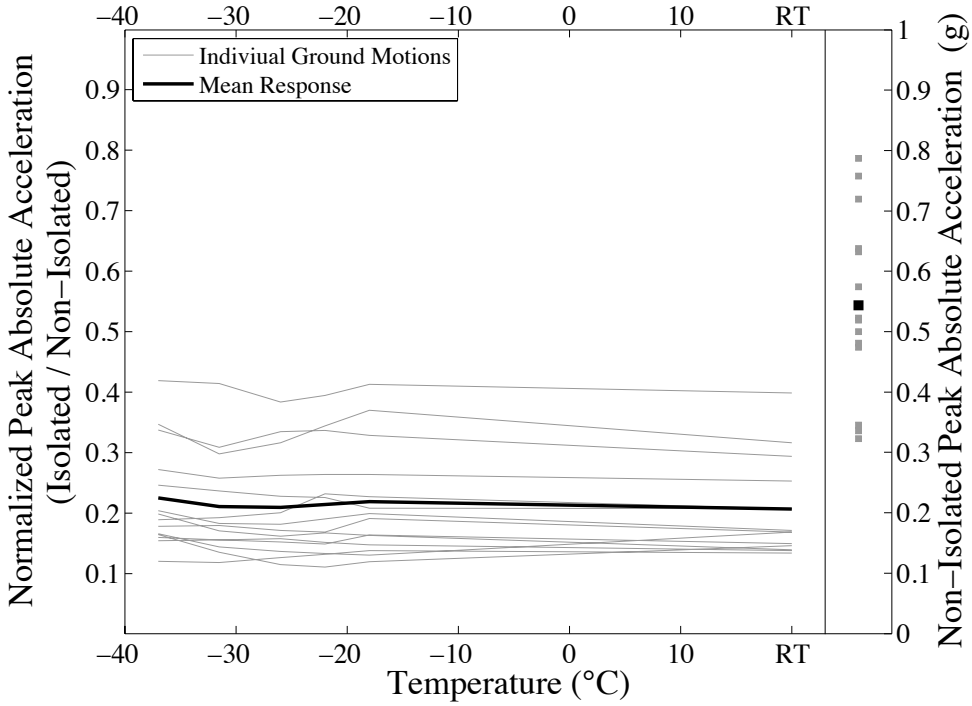

Figure 3.9: The change in peak absolute acceleration associated with low temperature conditioning for one day.

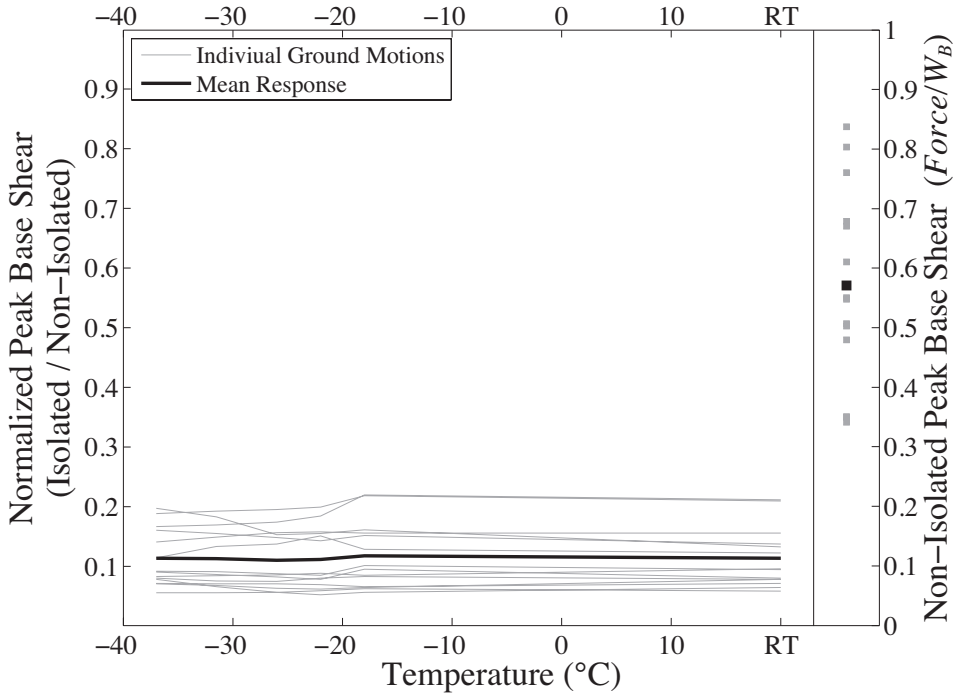

Figure 3.10: The change in peak base shear associated with low temperature conditioning for one day.

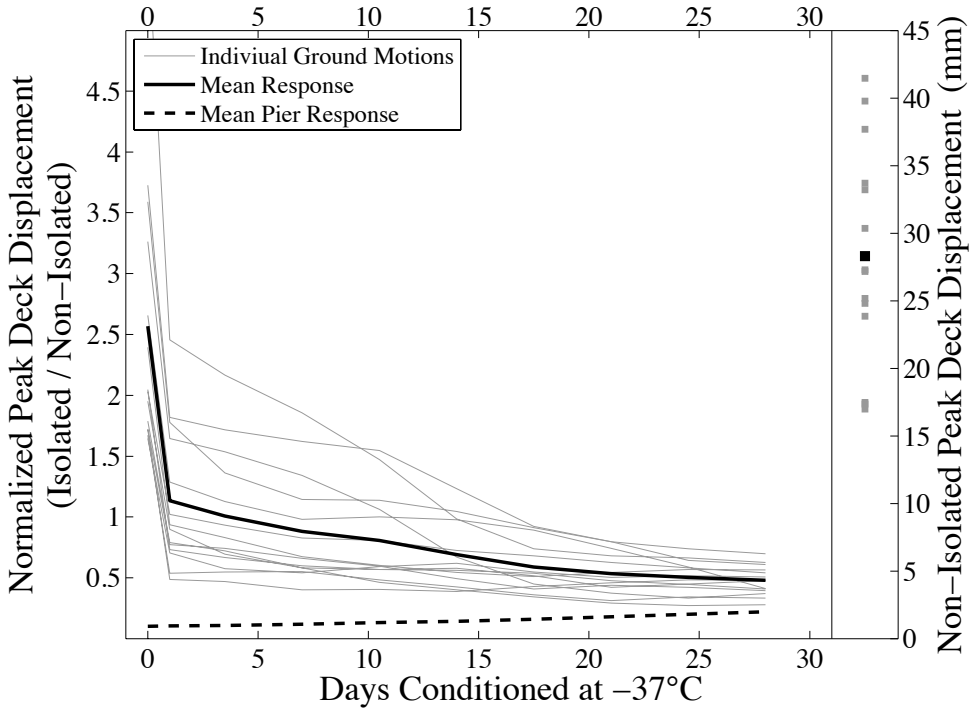

Figure 3.11: The change in peak deck displacement associated with low temperature conditioning at -37°C.

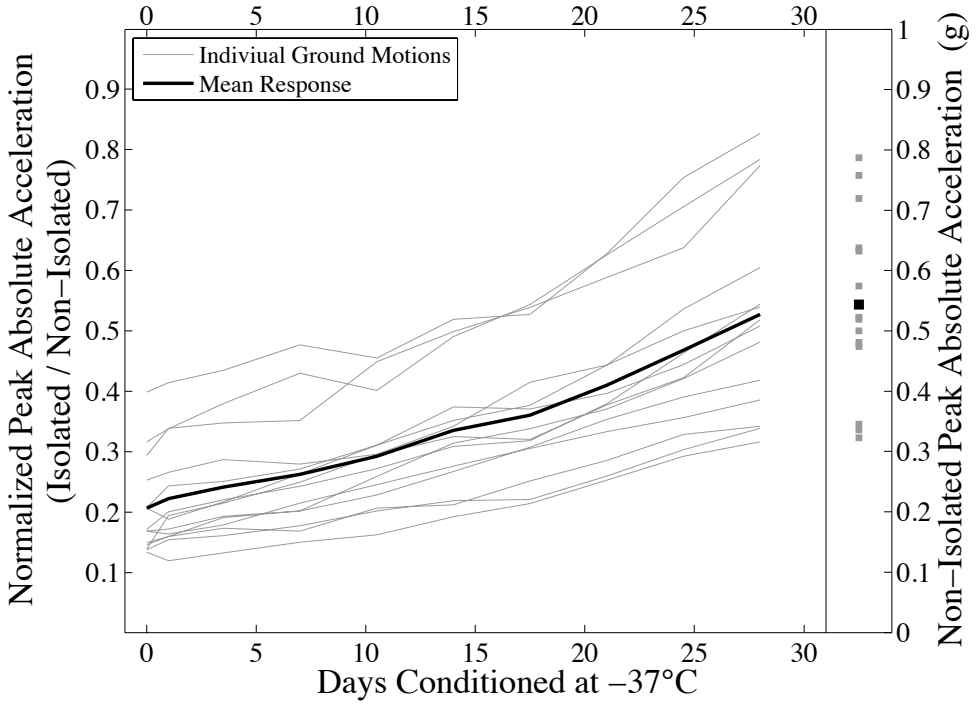

Figure 3.12: The change in peak absolute acceleration associated with low temperature conditioning at -37°C.

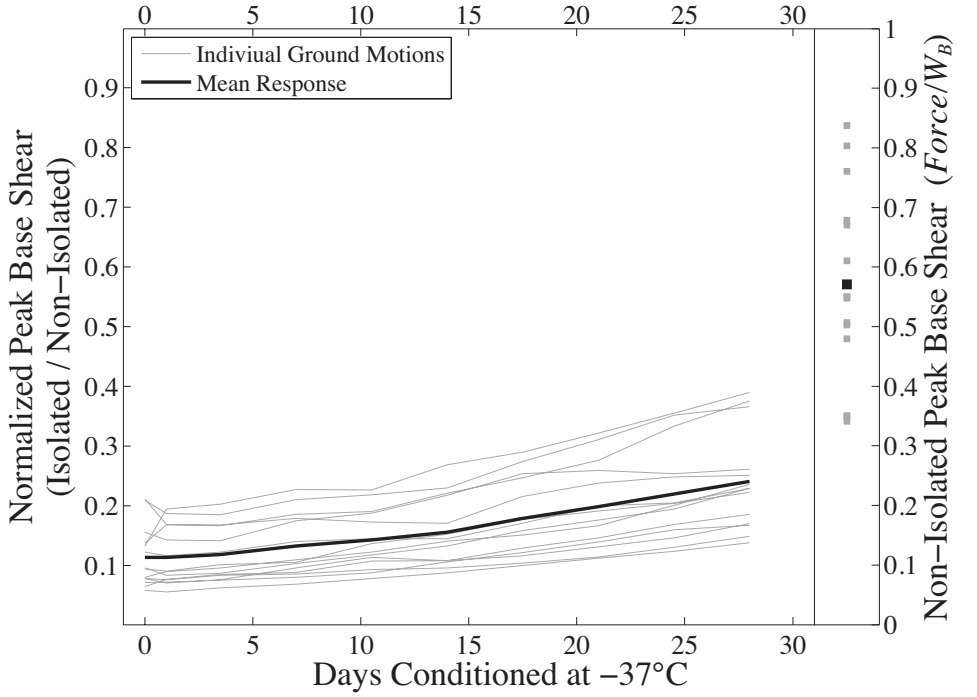

Figure 3.13: The change in peak base shear associated with low temperature conditioning at -37°C.

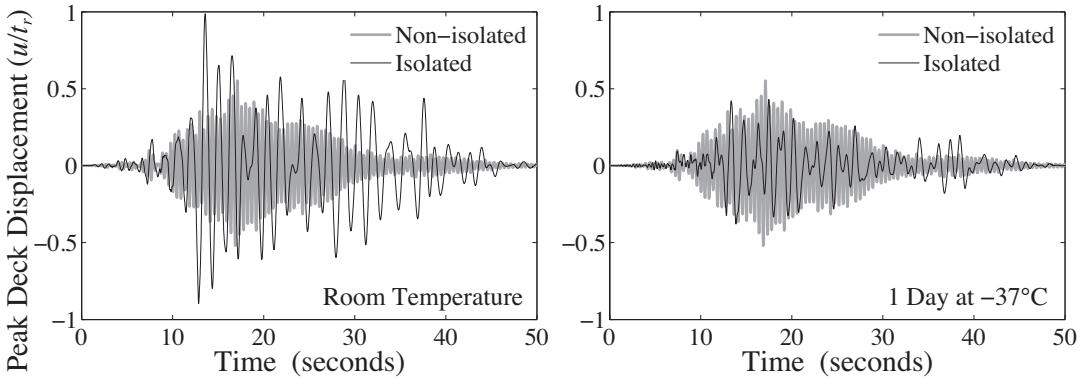

Figure 3.14: Deck displacement time history comparison for Chuetsu-oki, Japan ground motion.

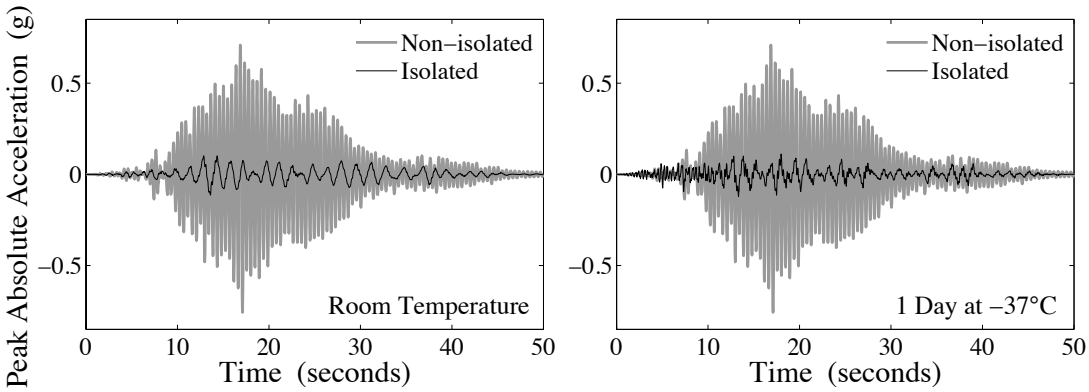

Figure 3.15: Absolute acceleration time history comparison for Chuetsu-oki, Japan ground motion.

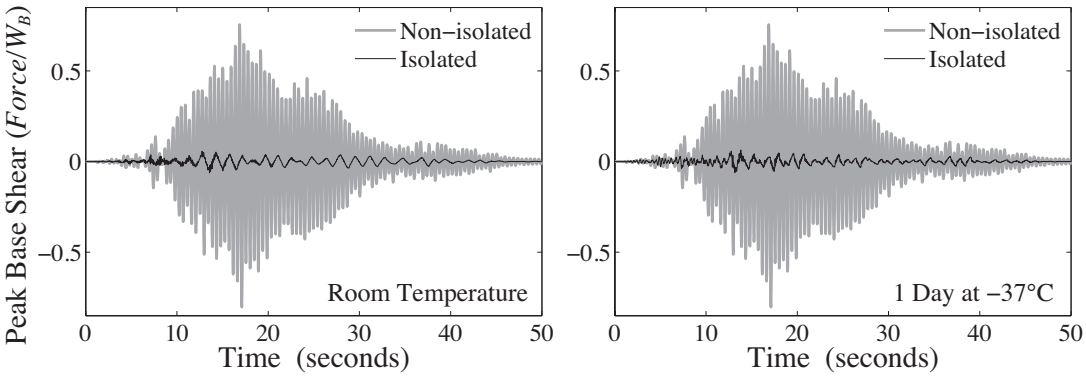

Figure 3.16: Base shear time history comparison for Chuetsu-oki, Japan ground motion.

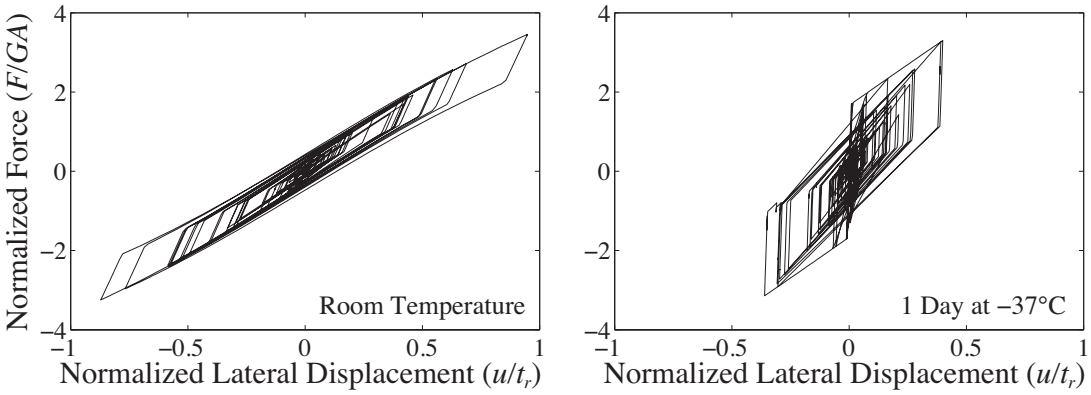

Figure 3.17: Isolator hysteretic behaviour comparison for Chuetsu-oki, Japan ground motion.

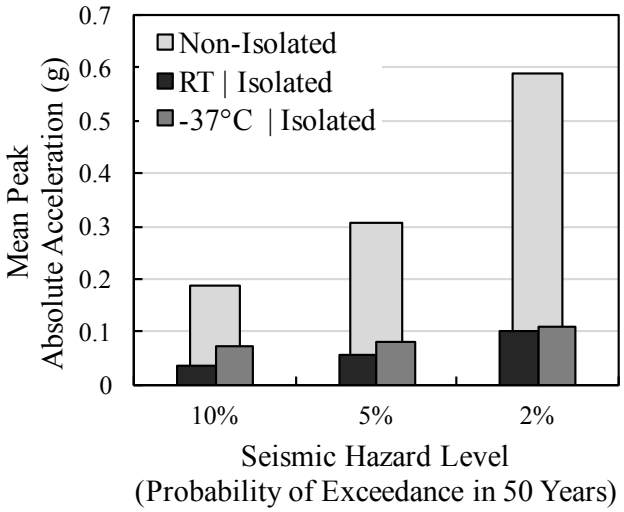

Figure 3.18: Mean peak absolute acceleration response comparison of all 14 ground motions.

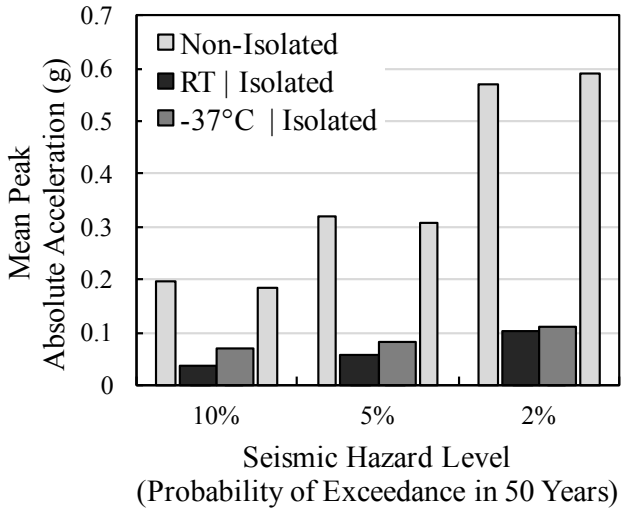

Figure 3.19: Mean peak normalized base shear response comparison of all 14 ground motions.

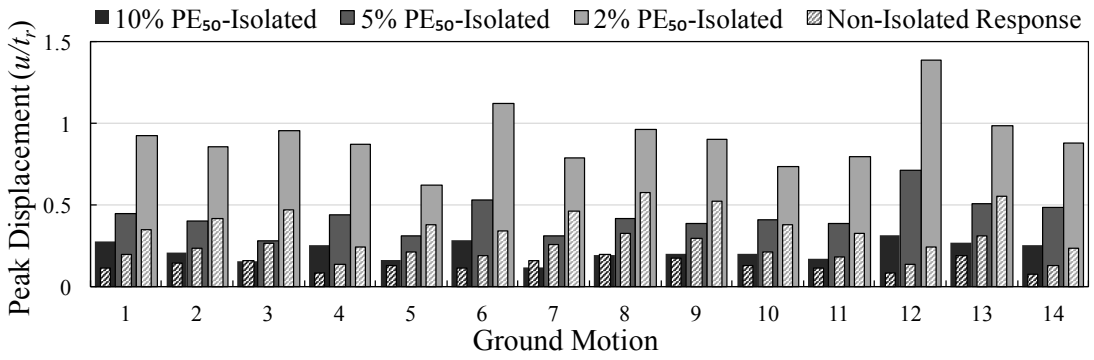

Figure 3.20: Peak isolator displacement response comparison between the room temperature isolated bridge and the non-isolated bridge for each hazard level.

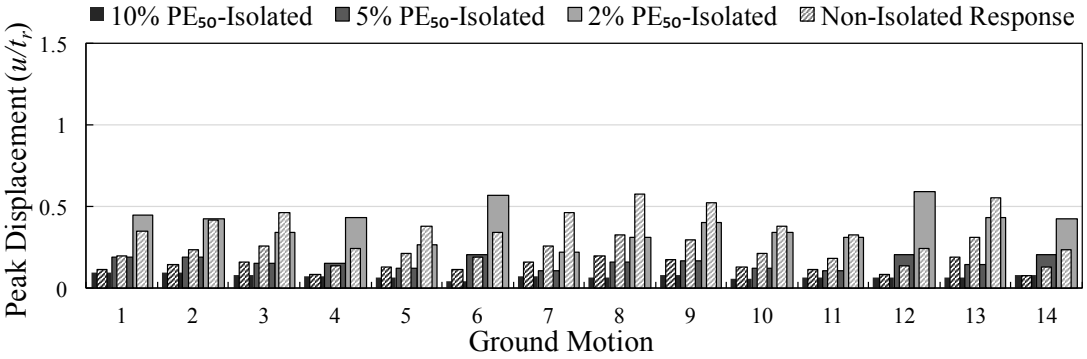

Figure 3.21: Peak isolator displacement response comparison between the isolated bridge at -37°C and the non-isolated bridge for each hazard level.

CHAPTER 4

CONCLUSIONS AND RECOMMENDATIONS

4.1 SUMMARY

Unbonded fiber-reinforced elastomeric isolators (U-FREI) are a relatively new type of isolator that have been shown to be viable for bridge applications. They can be employed as a bridge bearing to accommodate loads typically expected during normal operation of the bridge, but can also provide seismic isolation in the event of an earthquake. In order to be used with bridges located in cold northern climates, U-FREI must be able to provide acceptable performance at low temperatures. The effects of low temperatures on elastomeric isolators have been shown to cause potentially large increases in stiffness. This increase in stiffness becomes greater as the temperature is decreased and the conditioning duration is extended (Roeder et al. 1990; Sciascetti and Tait 2017). This change is concerning for elastomeric isolation systems in general because they are expected to provide a layer of low stiffness that can accommodate displacements during seismic events. If the stiffness of the isolation layer is too large, the seismic demand is transferred from the isolator into the piers and bridge. Displacements are then accommodated at the expense of plastic deformation in the piers (Roeder et al. 1989).

Previous studies have explored the effect of temperature on the lateral response of elastomeric bridge bearings. However, these studies only examined displacement amplitudes typical of what would be expected from expansion and contraction in the bridge deck (Roeder et al. 1989; Yakut et al. 2002; Pinarbasi et al. 2007). U-FREI are

unbonded isolators thus, they must be able to withstand larger displacements than typical bridge bearings in order to effectively seismically isolate a bridge. In the unbonded application, FREI form a rollover mechanism as lateral displacements increase (Toopchi-Nezhad et al. 2008). Under ambient room temperatures, the rollover mechanism provides a decrease in effective lateral stiffness at low to moderate displacement amplitudes. For low temperature applications, this mechanism could prove to be beneficial in counteracting some of the increase in stiffness due to low temperature stiffening mechanisms. In addition, U-FREI are able to exhibit lift-off during rotational tests (Al-Anany and Tait 2015). As stiffness in the isolators increase, the onset of lift-off occurs at smaller angles of rotation. Compared to bonded bearings, the ability for the loading support to partially lift off of the isolator can prevent damage. As such, the increased stress caused by tension in the elastomer, which would have been present in the bonded variant, can be significantly reduced (Al-Anany and Tait 2015).

In order to investigate the effects of low temperature on U-FREI and to confirm their effectiveness as both a bearing and a seismic isolator, an experimental program was developed in this study. A set of 28 U-FREI specimens were manufactured with the ability to exhibit a stable rollover mechanism. These isolators were conditioned at temperatures of -18°C, -26°C and -37°C for durations of 1, 14 and 28 days. The 1 day durations provided information on the effect of instantaneous thermal stiffening, while the 14 and 28 day tests provided information on the effect of crystallization on the elastomer. The specimens were separated into three sets of isolators that were tested

under one of three procedures: dynamic lateral displacements, vertical cyclic loading or cyclic rotations.

4.2 CONCLUSIONS

4.2.1 U-FREI as a Bridge Bearing

As a bridge bearing, the U-FREI specimens performed well at low temperatures without any damage. Under vertical cyclic loading, there was typically small change in stiffness or energy dissipation after 1 day of conditioning. A noticeable change was only seen for specimens subjected to -37°C for 14 and 28 days. Even during these tests, a maximum increase in stiffness of only 1.8 times the room temperature value was attained. As explained previously, an increase in vertical stiffness without any damage to the bearing is beneficial. The vertical frequency of the bearing increases as a result and rocking motions that could be instilled into the bridge are more likely to be prevented.

Under cyclic rotations, none of the specimens experienced any damage due to the FREI specimens being unbonded. Again, increases in stiffness were small for all specimens except the two U-FREI that were subjected to -37°C for 14 and 28 days. As expected at these conditions, the specimens exhibited lift-off due to the increase in stiffness from crystallization. The benefits could be seen in the rotational stiffness. At larger rotations, the stiffness decreased significantly, allowing the larger rotations to be accommodated. As a result, the largest increase that the specimens reached was limited to 2.4 times the room temperature value.

The experimental results indicate that, for use as a bridge bearing at low temperature, U-FREI are a viable option. Instantaneous thermal stiffening at temperatures reaching -37°C had little effect on the isolators. U-FREI can provide performance comparable to room temperature specimens during short term changes in temperature. Crystallization only had an effect on isolators at -37°C. Yet, it did not prevent U-FREI from providing acceptable performance during long term exposure to low temperatures.

4.2.2 U-FREI as a Seismic Isolator

As a seismic isolator, the main restriction for U-FREI is a limit imposed on the increase in stiffness allowed at low temperatures. During lateral testing, elastomeric isolators cannot increase in stiffness by more than four times the values obtained at room temperature. Every U-FREI, except one, easily passed this criterion; the largest increase in stiffness was only three times room temperature values. The specimen subjected to the harshest conditioning of 28 days at -37°C did not meet the imposed restriction, with an increase in stiffness of six times its room temperature values. Accompanying these increases in stiffness were even larger increases in dissipated energy. This caused a decrease in the damping ratio compared to the 1 and 14 day specimens at -37°C, but was still approximately 1.7 greater than the corresponding room temperature value.

Once it was determined that the U-FREI specimens can provide acceptable lateral performance at low temperature, an existing, non-iterative isolator model was updated using the test results to account for low temperatures. Two sets of equations

were developed in this process. The first equation set is a function of temperature that produces the parameters required to describe the effects of instantaneous thermal stiffening over the range of -18°C to -37°C. The second equation set is a function of conditioning duration at -37°C and describes the effects of crystallization on U-FREI over a period of 1 to 28 days. This updated isolator model was implemented into a numerical model of a three-span bridge in order to determine how isolators conditioned at low temperatures affect the response parameters of the bridge. A suite of 14 strong ground motions were used, scaled to the Uniform Hazard Spectra of Montreal, Quebec. Montreal was chosen as it is the largest city in Canada that experiences both low temperatures and high seismicity.

The results of the simulations provided verification that U-FREI are a viable type of seismic isolator for bridge structures at low temperatures. After 1 day of conditioning, a large reduction in peak deck displacement was found. This value was 1.1 times larger than the non-isolated bridge, while the displacement of the pier-top experienced a 90% reduction. Additionally, only minimal differences in peak absolute acceleration and base shear were observed compared to the room temperature isolated bridge. From these results, it is evident that the bridge was still effectively isolated after 1 day of conditioning down to -37°C. Further simulations where the bridge and U-FREI were conditioned for 28 days at -37°C had larger effects on the response parameters. The peak deck displacement continued to decrease to 48% of the non-isolated bridge. However, the peak base shear only gradually increased, staying well below 30% of the non-isolated values. The largest change was in the peak absolute acceleration, which

jumped from 20% to almost 55% of the non-isolated values. At this conditioning duration and temperature, the results from the experimental program had indicated that the U-FREI specimen did not pass the maximum stiffness increase criterion. Despite this, simulations have shown that low temperature U-FREI provide performance that exceeds that of a non-isolated bridge. As a result, strong ground motion simulations indicate that U-FREI, at *all* conditioning temperatures and durations from the experimental program, are viable for use as seismic isolators at low temperatures.

4.3 RECOMMENDATIONS

Through the experimental and numerical studies presented, it was determined that U-FREI are capable of providing acceptable performance at low temperatures. It is recommended that future studies on the topic further investigate U-FREI behaviour under other scenarios typically experienced by bridge bearings.

The specimens were tested separately under lateral, vertical and rotational loading. As a result, further tests examining the response of U-FREI under combined loading conditions would be beneficial. Most scenarios encountered at low temperatures involve lateral displacements due to bridge deck expansion and contraction. Some of these tests could include vertical cyclic loading under a fixed lateral deformation or cyclic rotation under a fixed lateral displacement. During periods of high volume on the bridge or during traffic, temporary fixed rotations could be imposed on the bearing. Further testing is proposed to investigate the response of lateral cyclic displacement under a fixed rotation or vertical cyclic loading under a fixed rotation.

In addition, this research was completed for isolators of identical properties. Valuable information could be obtained in carrying out the experimental program again, but as a parametric study where the physical properties of the isolators are changed. Variables that could be tested include: shape factor, aspect ratio as well as the number of layers in the isolator. Ultimately, however, a full-scale test should be completed in order to verify the scaling assumption that was used in creating the numerical model.

The numerical model provided a single example of the seismic performance of U-FREI in a bridge application. As a result, the findings from the numerical study are not general and are limited to the bridge that was modeled. It is recommended that more comprehensive results be obtained by completing the study with additional bridge configurations.

4.4 CLOSURE

The results provided herein are evident that U-FREI can provide acceptable performance when subjected to low temperature conditioning. Although further testing has been recommended, these studies provide confirmation that U-FREI can be a viable option for use as both bridge bearings and seismic isolators.

4.5 REFERENCES

Al-Anany, Y.M., and Tait, M.J. 2015. "A Numerical Study on the Compressive and Rotational Behaviour of Fiber Reinforced Elastomeric Isolators (FREI)." *Composite Structures* 133. Elsevier Ltd: 1249–66.

Pinarbasi, S., Akyuz, U., and Ozdemir, G. 2007. "An Experimental Study On Low Temperature Behavior Of Elastomeric Bridge Bearings." In *10th World Conference on Seismic Isolation, Energy Dissipation and Active Vibrations Control of Structures*. Istanbul, Turkey.

Roeder, C.W., Stanton, J., and Feller, T. 1989. "Low Temperature Behaviour and Acceptance Criteria for Elastomeric Bridge Bearings." Washington, D.C., USA: Transportation Research Board.

Roeder, C.W., Stanton, J., and Feller, T. 1990. "Low-Temperature Performance of Elastomeric Bearings." *Journal of Cold Regions Engineering* 4 (3): 113–32.

Sciascetti, A.N., and Tait, M.J. 2017. "The Effect of Temperature on the Lateral, Vertical and Rotational Response of Unbonded Fiber-Reinforced Elastomeric Isolators."

Toopchi-Nezhad, H., Tait, M.J., and Drysdale, R.G. 2008. "Testing and Modeling of Square Carbon Fiber-Reinforced Elastomeric Seismic Isolators." *Structural Control and Health Monitoring* 15: 876–900.

Yakut, A., Yura, J.A. 2002. "Parameters Influencing Performance of Elastomeric Bearings at Low Temperatures." *Journal of Structural Engineering* 128 (8): 986–94.